Short title: Ascorbate deficiency and NPQ in Chlamydomonas

Corresponding author:

Szilvia Z. Tóth

ORCID: https://orcid.org/0000-0003-3419-829X

e-mail: toth.szilviazita@brc.mta.hu

Title:

Ascorbate deficiency does not limit non-photochemical quenching in *Chlamydomonas reinhardtii*

Authors:

André Vidal-Meireles[1], Dávid Tóth[1,2], László Kovács[1], Juliane Neupert[3], Szilvia Z. Tóth[1]*

[1]Institute of Plant Biology, Biological Research Centre, Szeged, Hungary

[2]Doctoral School of Biology, University of Szeged, Szeged, Hungary

[3]Max-Planck Institut für Molekulare Pflanzenphysiologie, Potsdam-Golm, Germany

One-sentence summary:

In Chlamydomonas -in contrast to seed plants-, ascorbate is not required for violaxanthin deepoxidation and energy-dependent non-photochemical quenching but it mitigates photoinhibitory quenching.

Footnotes:

Author contributions: A. V.-M., J. N. and D. T. characterized the *Crvtc2-1* mutant and generated the complementation lines. L. K. developed the carotenoid content determination method. A. V.-M. performed the chl *a* fluorescece measurements, western blot analyses, and ascorbate content measurements. S. Z. T. conceived the study, analyzed the data and wrote the paper. A. V.-M. L. K. and J. N. contributed to analyzing the data and to the writing of the paper.

Funding:

This work was supported by the Lendület/Momentum Programme of the Hungarian Academy of Sciences (LP-2014/19), the National, Research and Development Office (NN 114524, GINOP-2.3.2-15-2016-00026) and the Alexander von Humboldt Foundation (grants to S Z T). A V-M received fellowships from the SEB / Company of Biologists Travel Fund, US DOE Travel Award and from the International Society of Photosynthesis Research (sponsored by Wiley on behalf of Plant, Cell and Environment).

Email address of author for contact:

toth.szilviazita@brc.hu (Szilvia Z. Tóth)

Summary

Ascorbate (vitamin C) plays essential roles in development, signaling, hormone biosynthesis, regulation of gene expression, stress resistance and photoprotection. In vascular plants, violaxanthin de-epoxidase (VDE) requires ascorbate (Asc) as reductant, thereby it is required for the energy-dependent component of non-photochemical quenching (NPQ). In order to assess the role of Asc in NPQ in green algae, which are known to contain low amounts of Asc, we searched for an insertional *Chlamydomonas reinhardtii* mutant affected in the *VTC2* gene, essential for Asc biosynthesis. The *Crvtc2-1* knockout mutant was viable and, depending on the growth conditions, it contained 10 to 20% Asc relative to its wild type. When Chlamydomonas was grown photomixotrophically at moderate light, the zeaxanthin-dependent component of NPQ emerged upon strong red illumination both in the *Crvtc2-1* mutant and in its wild type. Deepoxidation was unaffected by Asc deficiency, demonstrating that the Chlorophycean VDE found in Chlamydomonas does not require Asc as a reductant. The rapidly induced, energy-dependent NPQ component, characteristic of photoautotrophic Chlamydomonas cultures grown at high light, was not limited by Asc deficiency either. On the other hand, a reactive oxygen species-induced photoinhibitory NPQ component was greatly enhanced upon Asc deficiency, both under photomixotrophic and photoautotrophic conditions. These results demonstrate that Asc has distinct roles in NPQ formation in Chlamydomonas than in vascular plants.

Introduction

Ascorbate is a multifunctional metabolite, essential for a range of cellular processes in green plants, including cell division, stomatal movement, the synthesis of various plant hormones, epigenetic regulation and reactive oxygen species (ROS) scavenging (Asada, 2006; Foyer and Shigeoka, 2011; Smirnoff, 2018). Within the chloroplast, Asc may also act as an alternative electron donor to photosystem II (PSII) and to PSI (Ivanov et al., 2007; Tóth et al., 2009; Tóth et al., 2011). In vascular plants, violaxanthin de-epoxidase (VDE) requires ascorbate as reductant, thereby Asc plays an essential role in the process of non-photochemical quenching (NPQ) to dissipate excess energy as heat (Bratt et al., 1995; Saga et al., 2010; Hallin et al., 2016).

In order to fulfill the multiple physiological roles of Asc (reviewed by Tóth et al., 2018; Smirnoff, 2018), vascular plants maintain their Asc concentration at a high, approximately 20 to 30 mM level (Zechmann et al., 2011), which is also relatively constant, usually with no more than two-fold increase upon stress treatments and moderate decrease during dark periods (Dowdle et al., 2007). Notwithstanding, Asc concentration may be limiting under environmental stress conditions, as shown by an increased oxidative stress tolerance of plants overexpressing dehydroascorbate reductase, playing an essential role in Asc regeneration (Wang et al., 2010). Regarding NPQ, it was shown that Asc-deficient Arabidopsis plants have slowly inducible and diminished NPQ, whereas Asc-overproducing plants possess enhanced NPQ relative to wild type plants, meaning that Asc may limit the conversion of violaxanthin to zeaxanthin *in vivo* (Müller-Moulé et al., 2002; Tóth et al., 2011). Ascorbate deficient plants are also sensitive to high light, especially in combination with zeaxanthin deficiency (Müller-Moulé et al., 2003).

Green algae, for instance *Chlamydomonas reinhardtii*, produce Asc in a very small amount under favorable environmental conditions (approx. 100 to 400 µM, Gest et al., 2013), and boost it only in case of need, for instance upon a sudden increase in light intensity and in nutrient deprivation (Vidal-Meireles et al., 2017; Nagy et al., 2018). The mode of regulation of Asc biosynthesis differs largely between plants and Chlamydomonas: in contrast to vascular plants, i) green algal Asc biosynthesis is directly regulated by ROS, ii) it is not under circadian clock control and, iii) instead of a negative feedback regulation, there is a feedforward mechanism on the expression of the key Asc biosynthesis gene, *VTC2* (*Cre13.g588150*) by Asc in the physiological concentration range (Vidal-Meireles et al., 2017).

Regarding NPQ, it was described that the violaxanthin deepoxidase found in Chlorophyceae (CVDE) is not homologous to plant VDE but related to a lycopene cyclase of photosynthetic bacteria (Li et al., 2016a). Chlamydomonas CVDE (CrCVDE), encoded by *Cre04.g221550*, has a FAD-binding domain and it is located on the stromal side and not in the thylakoid lumen, as it is the case for plant-type VDE (Li et al., 2016a). The cofactor or reductant requirement of the CrCVDE enzyme has not been investigated, and it is not known whether its activity requires Asc, either directly or indirectly.

Due to the major differences in Asc contents, the regulation of Asc biosynthesis and the VDE enzymes of vascular plants and Chlorophyceae, we decided to assess the role of Asc in the various NPQ components in *Chlamydomonas reinhardtii*. To this end, we characterized an insertional *VTC2* mutant procured from the CLiP library (Li et al., 2016b), possessing only 10 to 20% Asc relative to its parent strain. We have found that, in contrast to vascular plants, Asc deficiency does not limit energy-dependent quenching (qE) and violaxanthin de-epoxidation in Chlamydomonas; instead, Asc deficiency leads to enhanced photoinhibitory quenching (qI) upon excessive illumination.

Results

Identification and initial characterization of an Asc-deficient VTC2 insertional mutant of C. reinhardtii and its genetic complementation

To investigate the function of Asc in NPQ in *C. reinhardtii*, we searched for insertion mutants for the *VTC2* gene in the CLiP library (Li et al., 2016b). We found one putative *VTC2* mutant (strain *LMJ.RY0402.058624*, hereafter called *Crvtc2-1*), holding one insertion of the paromomycin resistance (CIB1) casette at the junction site of exon 3 and the adjacent upstream intron of the *VTC2* gene (Fig. 1A). The other available mutants were affected in the 3'UTR region of the *VTC2* gene and/or had multiple insertions in genes other than *VTC2*. One of the strains carrying a CIB1 casette in the 3'UTR region of the *VTC2* gene with an insertion confidence of 95% (*LMJ.RY0402.146784*) was tested, but we found that it had wild-type level Asc content (data not shown); therefore, it was not used for further analyses. Due to the lack of another, independent CIB insertional mutant line affecting only the *VTC2* gene, we carried out several NPQ measurements on our previously published *VTC2*-amiRNA line (Vidal-Meireles et al., 2017) to confirm our findings on the consequences of Asc deficiency on NPQ (see below).

The site of CIB1 casette integration in the CLiP mutants had been validated by LEAP-Seq method (Li et al., 2016b), and we verified it in the *Crvtc2-1* mutant by PCR (Fig. 1B). Using primers annealing upstream the predicted insertion site in *VTC2*, a specific 852 bp fragment was observed in genomic DNA samples isolated from wild type *C. reinhardtii* cells (CC-4533) and from the *Crvtc2-1* mutant strain (Fig. 1B, top panel); using primers designed to amplify the 5' and 3' junction sites of the CIB1 cassette, specific 470 and 601 bp fragments could be detected in the *Crvtc2-1* mutant (Fig. 1B, middle and bottom panels).

Sequencing analysis of the PCR amplicons confirmed the predicted insertion of the CIB1 cassette in antisense orientation with its 5' junction in the third exon of the gene and the 3' junction reaching to the adjacent intron upstream of exon 3 (Supplemental Fig. S1).

Under moderate light (100 µmole photons m^{-2} s^{-1}) and photomixotrophic conditions (growth in Tris-acetate-phosphate (TAP) medium), the wild type strain (CC-4533) had approx. 12 pmol Asc/ µg Chl(a+b) (Fig. 1C), corresponding to about 200 µM cellular Asc concentration (see Kovács et al., 2016 for calculations), and the *Crvtc2-1* mutant had a very low Asc content, only approx. 10% of the wild type. When the cultures were treated with 1.5 mM H_2O_2, which had been shown to result in a strong increase in Asc content (Urzica et al., 2012; Vidal-Meireles et al., 2017), the Asc content in the wild type increased approximately three-fold, whereas in the *Crvtc2-1* mutant it did not increase (Fig. 1C). This is in contrast to the *VTC2*-amiRNA lines generated earlier, where H_2O_2 treatment resulted in noticeable Asc accumulation (Vidal-Meireles et al., 2017).

Via real time qRT-PCR analysis with primers located upstream and downstream of the insertion site of the CIB1 cassette no *VTC2* transcript could be detected in the *Crvtc2-1* mutant samples, grown under normal growth conditions or treated with H_2O_2 (Fig. 1D). Similarly, in qRT-PCR analysis using primers spanning the sequence encoding the catalytic site of *VTC2* (which is located downstream of the CIB1 casette insertion site), no transcript could be detected in the *Crvtc2-1* mutant under normal growth conditions, and only a weak signal could be observed upon 35 PCR cycles in the H_2O_2-treated *Crvtc2-1* mutant samples (Fig. 1E).

In order to confirm that the decrease in Asc content is caused by the functional deletion of *VTC2* in the insertional mutant strain, genetic complementation was carried out. To this end, we transformed the *Crvtc2-1* insertional mutant with the coding sequence of *VTC2*, controlled by the constitutive promoter *PsaD*. The plasmid used for transformation

included the *APH7"* resistance gene (Fig. 2A), thus the ability to grow on a medium containing hygromycin-B was used as the first screening method for successful transformation.

The integration of the plasmid in the genome was verified by PCR. Using a forward primer annealing to the *PSAD* promoter region and a reverse primer annealing to the 5' end of the *VTC2* coding sequence, a specific 841 bp fragment could be amplified in genomic DNA samples isolated from two independent complementation lines of *Crvtc2-1+VTC2* (Fig. 2B). The *VTC2* transcript could be detected in the complemented *Crvtc2-1+VTC2* lines via qRT-PCR analysis with primers spanning the sequence encoding the catalytic site (Fig. 2C). The Asc content of the complementation lines were restored to a great extent (Fig. 2D). The cell volume, the cellular Chl content and Chl*a/b* ratios were moderately increased in the *Crvtc2-1* mutant relatively to the wild type and these parameters were partially restored upon complementation (Supplemental Fig. S2A, B, C).

Regarding the growth phenotypes, no significant difference was observed between the strains when grown in TAP medium at 100 µmole photons m^{-2} s^{-1}, whereas the growth of the *Crvtc2-1* mutant was severely inhibited in TAP medium at 530 µmole photons m^{-2} s^{-1}, which was restored upon genetic complementation. In HSM medium at 530 µmole photons m^{-2} s^{-1} growth was slow in all genotypes and no significant differences were observed among them (Supplemental Fig. S2D). The Asc content increased two- to three-fold in each strains upon high light treatment, and the Asc content of the *Crvtc2-1* mutant remained at a level of 10-20% relative to the wild type and the complementation lines (Supplemental Fig. S2E).

The effects of Asc deficiency on NPQ in cultures grown at normal light and photomixotrophic conditions

NPQ includes short-term responses to changes in light intensity, as well as responses that occur over longer periods allowing for acclimation to high light exposure. In *C. reinhardtii*, the levels of the different NPQ components are variable and highly dependent on the growth conditions (Niyogi et al., 1997; Finazzi et al., 2006; Iwai et al., 2007; Peers et al 2009).

In a first set of experiments to assess the effects of Asc deficiency on NPQ, Chlamydomonas strains were cultured in TAP medium, at 100 µmol photons m^{-2} s^{-1}. Before the NPQ measurements, cultures were dark-adapted for about 30 min with shaking in order to avoid anaerobiosis; this dark adaptation protocol ensures the relaxation of most NPQ processes and the separation of the NPQ components induced under high light illumination (Roach and Na, 2017). When subjecting the cells to continuous red light of 530 µmol photons m^{-2} s^{-1}, a small, rapidly induced NPQ component was induced in the wild type and the Asc-deficient *Crvtc2-1* strain in the first 2 min (Fig. 3A), that we attribute to energy-dependent component (qE). qE is activated by low lumen pH, which occurs for instance during the induction of photosynthesis and upon CO_2 limitation of the Calvin-Benson-Bassham cycle (Kanazawa and Kramer, 2002; Takizawa et al., 2008). In *C. reinhardtii*, qE formation also requires zeaxanthin or lutein (Ericksson et al., 2015) and it is enhanced by a stress-related LHC protein, LHCSR3, which is strongly expressed when algae are grown at high light (Xue et al., 2015; Peers et al., 2009; Bonente et al., 2011; Chaux et al., 2017). At moderate light (100 µmol photons m^{-2} s^{-1}) and photomixotrophic growth conditions, LHCSR3 level was relatively low, particularly in the *Crvtc2-1* strain (Supplemental Fig. S3). The presence of acetate also enables high Calvin-Benson-Bassham cycle activity and a relatively low qE (Johnson and Alric, 2012), in agreement with our findings.

A slower NPQ component, induced on the timescale of several minutes was also present, which was enhanced in the Asc-deficient *Crvtc2-1* mutant (Fig. 3A) and restored in its complementation strains (Supplemental Fig. S4A). This slow component was enhanced in

our previously published *VTC2*-amiRNA line relative to its control strain as well (Supplemental Fig. S4C).

Three components may be responsible for this slowly induced NPQ component (see Ericksson et al., 2015; Allorent et al., 2013): i) zeaxanthin dependent quenching, which may act on NPQ directly (e.g. Holt et al., 2005; Holub et al., 2007; Avenson et al., 2008) or indirectly by controlling the sensitivity of qE to the pH gradient or promoting conformational changes within LHCs (e.g. Johnson et al., 2008; Ruban et al., 2012); ii) State transition-dependent quenching (qT), which may contribute to balancing excitation energy between PSII and PSI via LHCII phosphorylation and antenna dissociation from PSII (Depège, 2003; Lemeille et al., 2009; Ünlü et al., 2014); iii) A slowly relaxing, "photoinhibitory" quenching (qI), associated with photosystem II (PSII) damage or slowly reversible downregulation of PSII representing a continuous form of photoprotection (Adams et al. 2013; Tikkanen et al., 2014).

In order to decipher the origin of the slow NPQ component and to study the possible role of Asc in NPQ, carotenoids were analyzed first, using HPLC. Upon illumination, the de-epoxidation index largely increased (from about 0.05 to 0.25) both in the CC-4533 (wild type) strain and the *Crvtc2-1* mutant, and de-epoxidation only moderately recovered after the cessation of actinic illumination in both strains (Fig. 3B). Violaxanthin, antheraxanthin and zeaxanthin concentrations were essentially the same in the *Crvtc2-1* mutant and in the wild type (Supplemental Fig. S5A, B, C). These results suggest that qZ was partially responsible for the slow NPQ component and that Asc deficiency does not limit the de-epoxidation reaction. We also found that the amounts of β-carotene and lutein were not affected by the lack of Asc and their quantities remained constant during the entire protocol (Supplemental Fig. S5D, E). The F_V/F_M values of dark-adapted cultures and those subjected to high light

237 illumination followed by a recovery period were also very similar, with no major differences
238 between the Asc-deficient mutant and the CC-4533 strain (Fig. 3C).

239 Since the de-epoxidation ratios were the same in the CC-4533 strain and in the
240 *Crvtc2-1* mutant (Fig. 3B), it is likely that Asc-deficiency does not limit the reaction. In order
241 to completely exclude this possibility, a 16-h dark acclimation experiment was carried out,
242 ensuring undetectably low level of Asc (Fig. 4A). Still, NPQ was induced slowly upon
243 illumination (Fig. 4B), and the de-epoxidation indices were similar than in cultures subjected
244 to relatively short dark adaptation (compare Fig. 4C and Fig. 3B); we note that during a 30-
245 min illumination Asc does not accumulate (Vidal-Meireles et al., 2017).

246 The large increase in the de-epoxidation index upon illumination suggests that qZ is at
247 least partially responsible for the slow NPQ component. However, we also observed that the
248 slow NPQ component was larger in the *Crvtc2-1* mutant than in the wild type, whereas the
249 de-epoxidation ratios were the same (Fig. 3A, B). In addition to qZ, qT and qI mechanisms
250 may also contribute to the slow component and they may differ between the wild type and the
251 *Crvtc2-1* mutant. The possible contribution of qT was studied by measuring 77K
252 fluorescence spectra: Upon illumination with 530 µmole photons $m^{-2}s^{-1}$ red light, the 684
253 nm/710 nm ratio remained unaltered in the wild type and increased slightly in the Asc-
254 deficient mutant (Fig. 3D). Transition from state I to state II would decrease the 684/710 nm
255 ratio, therefore, in our cultures grown at moderate light in TAP medium and subjected to
256 strong red illumination during the fluorescence measurement, qT is unlikely to contribute to
257 NPQ induction. On the other hand, when the actinic illumination was switched off, the
258 684/710 nm ratio decreased moderately, reflecting the occurrence of state I to state II
259 transition in the dark.

260 To further study the effect of state transition in the induction and relaxation of NPQ, a
261 state transition mutant, called *stt7-9* (Depège et al., 2003) was employed. NPQ was induced

during illumination in the *stt7-9* mutant to a similar extent as in the *Crvtc2-1* mutant (albeit with rather different kinetics), which coincided with a strong zeaxanthin accumulation (Supplemental Fig. S6B); this indicates that transition to state II did not play a role in the formation of NPQ under the present experimental conditions. On the other hand, upon the cessation of actinic illumination, there was a rapid NPQ relaxation in the *stt7-9* mutant, showing that transition to state II occurs in the wild types and the *Crvtc2-1* mutant in the dark, probably masking the relaxation of the other NPQ components.

As a next step, the effect of oxidative stress, known to enhance NPQ (Roach and Na, 2017), was tested by employing H_2O_2 and catalase treatments on the *Crvtc2-1* mutant and its wild type. Fig. 5A and B show that upon the addition of 1.5 mM H_2O_2, the slow NPQ component increased remarkably in both strains, without altering the de-epoxidation level (Fig. 5C). When 5 µg/ml catalase was added, NPQ was only slightly affected in the wild type (Fig. 5D), whereas it significantly decreased in the Asc-deficient mutant (Fig. 5E). These data suggest that H_2O_2 accumulated upon strong illumination in the Asc-deficient mutant, resulting in enhanced NPQ. On the other hand, the F_V/F_M value, an indicator of photosynthetic efficiency, did recover following illumination and to a similar extent in the wild type and the *Crvtc2-1* strain (Fig. 3C), thus photosynthetic reaction centers did not get severely inhibited.

For comparison, the *npq1* mutant, lacking the CVDE enzyme, thus unable to perform violaxanthin de-epoxidation (Niyogi et al., 1997), was also tested. Upon illumination with 530 µmol photons m^{-2} s^{-1}, this strain developed a large NPQ (Fig. 6A), which was accompanied by irreversible decrease of F_V/F_M and loss of Chl and β-carotene relative to its wild type (137a) strain (Fig. 6B, C, D). 77 K fluorescence recordings showed no changes in the 684nm/710nm ratio (Fig. 6E), thus the large NPQ component could be unambiguously attributed to photoinhibitory qI. Interestingly, the Asc concentration in the *npq1* mutant is

very high compared to the other strains (Fig. 6F), probably to compensate for the lack of CVDE and zeaxanthin in ROS management (Baroli et al., 2003). Thus, the experiments on the *npq1* mutant corroborate the importance of CVDE in strong illumination.

The effects of Asc deficiency on NPQ in cultures grown under photoautotrophic conditions at high and moderate light

When the cultures were grown under photoautotrophic conditions without CO_2 supplementation under strong white light (530 µmole photons $m^{-2}s^{-1}$), which was similar in intensity used for NPQ induction measurements, qE reached relatively high values (about 1.0) both in the wild type and the Asc-deficient CLiP mutant (Fig. 7A). In the *VTC2*-amiRNA line, the qE component was enhanced relative to its empty vector control (Supplemental Fig. S4D). These results show that Asc is not required for the formation of the qE component. The qE phase was followed by a slower one, which was enhanced both in the *Crvtc2-1* mutant and the *VTC2* amiRNA line relative to their control strains.

During illumination, the de-epoxidation index changed only marginally, and it was essentially the same in the wild type and in the Asc-deficient strain (about 0.1, Fig. 7B). The F_V/F_M value was also unaffected in the *Crvtc2-1* mutant relative to its wild type before or after the illumination with strong red light (Fig. 7C). The 684nm/710nm ratio of the 77 K spectra remained constant in the Asc-deficient mutant (Fig. 7D). The violaxanthin, antheraxanthin, zeaxanthin and lutein contents did not decrease upon illumination with intense red light in either strain (Supplemental Fig. S7), only the total amount of β-carotene was slightly lower in the Asc-deficient mutant (Supplemental Fig. S7D). We also observed that under high light growth conditions, the amount of photosynthetic complexes (namely PsbA, CP43, PSBO, PsaA, LHCSR3, PetB and RbcL) were essentially the same in the

311 *Crvtc2-1* mutant and in the wild type, as detected by western blot analysis on equal chl basis
312 (Supplemental Fig. S3).

313 Treatments with 1.5 mM H_2O_2 led to alteration of the NPQ kinetics and a slower
314 relaxation in both strains (Fig. 8A, B). In the *Crvtc2-1* mutant, catalase treatment resulted in a
315 strong decrease of qE and the slow NPQ component (Fig. 8C, D). These results show that
316 under photoautotrophic and high light conditions, Asc-deficiency does not limit qE or qZ but
317 may lead to the occurrence of oxidative stress and thereby to increased qI.

318 Subjecting the cells in HSM medium in moderate light (100 µmole photons $m^{-2}s^{-1}$)
319 resulted in similar effects in terms of qE, de-epoxidation, the 684/710 nm ratio of the 77 K
320 spectra and H_2O_2 and catalase responsiveness (Supplemental Fig. S8).

321

322 **Discussion**

323

324 *The Crvtc2-1 CLiP mutant possesses a low Asc content without major changes in the*
325 *phenotype*

326 *VTC2* encodes GDP-L-galactose phosphorylase, an essential and highly regulated enzyme of
327 Asc biosynthesis both in vascular plants and in green algae (Urzica et al., 2012; Vidal-
328 Meireles et al., 2017) and downregulating *VTC2* via the amiRNA technique results in Asc
329 deficiency (Vidal-Meireles et al., 2017). For the present study, we identified and genetically
330 complemented a *VTC2* mutant in the CLiP collection that carries a single insertion in the
331 *VTC2* gene (Fig. 1 and Fig. 2). The *Crvtc2-1* mutant possesses about 10% Asc relative to its
332 wild type strain CC-4533 under normal growth conditions, its Asc content is unaltered upon
333 H_2O_2 treatment and remains below 20% of the wild type under high light conditions; in
334 addition, by employing overnight dark acclimation, the Asc concentration of the *Crvtc2-1*
335 mutant strongly decreased (Fig. 4).

The *Crvtc2-1* mutant is very likely to be a knockout for *VTC2* as no transcript accumulation could be detected performing qRT-PCR with primers annealing downstream of the CIB cassette insertion site and spanning the sequence encoding the catalytic site of GDP-L-galactose phosphorylase. Only when the cultures were treated with H_2O_2 and when a high PCR cycle number was used (Fig. 1E) a faint band could be observed in the gel. It is very unlikely that a functional truncated GDP-L-galactose phosphorylase is present in the mutant, but the observation that the *Crvtc2-1* strain still contains 10-20% Asc relative to its parent strain suggests that some phosphorolysis of GDP-L-galactose could be carried out by another enzyme ensuring minor amount of Asc. We note that in Arabidopsis *VTC2* has a lowly expressed homologue, *VTC5*, and knocking out both of them results in seedling lethality (Dowdle et al., 2007). In Chlamydomonas, no homologue of *VTC2* has been identified (Urzica et al., 2012). On the other hand, it is possible that GDP-L-galactose is degraded hydrolytically (with L-galactose-1-P and GMP as products) leading to minor Asc production in the *VTC2* mutant. An alternative Asc biosynthesis pathway may also exist in Chlamydomonas, although homologues of enzymes possibly involved in alternative Asc biosynthesis pathways in vascular plants could not be found in Chlamydomonas (Urzica et al., 2012; Wheeler et al., 2015).

In spite of the very low Asc content of the *Crvtc2-1* mutant, the phenotype was only moderately altered. The *Crvtc2-1* mutant has the same growth rate than the wild type and the complementation lines at moderate light conditions in TAP medium (Supplemental Fig. S2). The amounts of various photosynthetic subunits were similar in the Asc-deficient *Crvtc2-1* mutant than in the wild type strain CC-4533 in TAP medium at moderate light and also in HSM medium both at moderate and high light (Supplemental Figure S3). Unexpectedly, the amount of the photoprotective LHCSR3 protein was reduced in the *Crvtc2-1* mutant in TAP medium at moderate light and it was at the same level than in the wild type when grown in

HSM medium both at medium and high light. The amounts of carotenoids are unchanged in the *Crvtc2-1* line in cultures grown at normal light, whereas at high light in HSM medium, the amount of β-carotene is slightly reduced (Supplemental Fig. S5 and S7). The *Crvtc2-1* line had a slightly higher Chl content than its wild type and cell size was also moderately increased (Fig. 2). A marked characteristics of the *Crvtc2-1* mutants was that it was unable to grow at high light in TAP medium (Supplemental Fig. S2).

In our previously published *VTC2*-amiRNA line Asc deficiency led to more severe alterations in the phenotype than it was observed in the *Crvtc2-1* mutant (Vidal-Meireles et al., 2017). The reason behind this remains to be elucidated, although the cell wall deficiency of the cw15-325 line (the parent strain of the *VTC2*-amiRNA line) and thereby its increased stress sensitivity (Voigt and Münzner, 1994) may explain the differences between the *VTC2*-amiRNA and the *Crvtc2-1* insertional mutant strains.

The effects of Asc deficiency on the qE component of NPQ

C. reinhardtii uses various photoacclimation strategies which strongly depend on the carbon availability and the trophic status of the cells (Polukhina et al., 2016). The fast rise in NPQ (qE) is enhanced upon growth at high light and low CO_2 that is enabled by a high expression of LHCSR3 (e.g. Peers et al., 2009). It has been observed that under photomixotrophic conditions at normal light, the expression of the LHCSR proteins is very low and qE is minor; in addition, the deepoxidation state is also known to vary with the growth light (Polukhina et al., 2016). Therefore, in order to study the role of Asc in the different NPQ parameters, we subjected the cultures both to moderate and high light, photomixotrophic and photoautotrophic conditions. As shown by our results and the discussion below, by these means we managed to distinguish between qE, qZ, and qI, and only qT could not be studied in detail.

Rapid response to changes in light intensity and dissipation of excess light energy are particularly important when the activity of the Calvin-Benson-Bassham cycle is limiting, in order to avoid a potentially deleterious buildup of excessive ΔpH (Kanazawa and Kramer, 2002; Takizawa et al., 2008). In agreement with the literature (Xue et al., 2015), at normal light and photomixotrophic conditions, the rapidly inducible qE was a minor component and the relative amount of the LHCSR3 protein, essential for qE development was low (Supplemental Fig. S3). When Chlamydomonas cultures were grown at photoautotrophic, possibly CO_2-limiting conditions, the amplitude of qE largely increased both at moderate and high light (Supplemental Fig S8 and Fig. 8, respectively) enabled by the accumulation of LHCSR3 (Supplemental Fig. S3) and possibly by other factors.

Our results on the *Crvtc2-1* line show that qE is not limited by Asc deficiency neither at low light nor at high light conditions, nor under photomixotrophic and photoautotrophic conditions; in the *VTC2*-amiRNA line, qE was even enhanced relative to its control line (Supplemental Fig. S4B).

The effects of Asc deficiency on the slow NPQ components

In Chlamydomonas, a slowly induced NPQ component, with several underlying mechanisms, may also be induced. When CC-4533 cultures were grown at normal light in TAP medium and subjected to strong red light, the major slow component was probably qZ, as shown by the large increase in de-epoxidation (Fig. 3) and by the loss of NPQ induction in the *npq1* mutant (Fig. 6). In cultures grown at high light and photoautotrophic conditions, de-epoxidation was minor upon light adaptation with strong red light (Fig. 7) and it was intermediate when the cultures were grown photoautotrophically at moderate light (Supplemental Fig. S8). De-epoxidation was equal in the *Crvtc2-1* mutant and the wild type in all growth conditions and also upon overnight dark acclimation that led to undetectably

411 low Asc content in the *Crvtc2-1* mutant. These results clearly show that Asc deficiency is not
412 limiting qZ, thus Asc is not used as a reductant by CrCVDE.

413 The xanthophyll cycle, in which violaxanthin is converted into zeaxanthin during light
414 acclimation, is ubiquitous among green algae, mosses and plants, with exception of
415 Bryopsidales, a monophyletic branch of the Ulvophyceaes in which NPQ is neither related to
416 a pH-dependent mechanism, nor modulated by the activity of the xanthophyll cycle (Christa
417 et al., 2017). It has also been shown that among green alga species, large variations exist in
418 the activity of xanthophyll cycle and in its overall contribution to NPQ, which seems to
419 depend on the environmental selection pressure and less on the phylogeny (Quaas et al.,
420 2015). In mosses, the xanthophyll cycle was shown to significantly contribute to excess
421 energy dissipation upon stress conditions (e.g. Azzabi et al., 2012).

422 The de-epoxidation reaction itself is catalyzed by distinct enzymes in vascular plants
423 and in Chlorophyceae, including Chlamydomonas (Li et al., 2016a). Plant-type VDE is
424 associated with the thylakoid membrane on the luminal side, where it catalyzes the de-
425 epoxidation reaction of violaxanthin, found in free lipid phase and it uses Asc as a reductant
426 (Hager and Holocher, 1994; Arnoux et al., 2009). CVDE is located on the stromal side of the
427 thylakoid membrane, and, just like higher plant VDE, it also requires a build-up of ΔpH for
428 its activity (Li et al., 2016a). CVDE is related to lycopene cyclases of photosynthetic bacteria,
429 called CruA and CruP (Li et al., 2016a, Bradbury et al., 2012). We have demonstrated in this
430 paper that Asc is not required for the de-epoxidation reaction, and, in general, for qZ in
431 Chlamydomonas.

432 Green algae contain very small amounts of Asc relative to vascular plants, and, as
433 stated above, effective de-epoxidation is achieved by an enzyme that does not require Asc as
434 a reductant. Interestingly, brown algae, which produce minor amounts of Asc as well,
435 diadinoxanthin de-epoxidase uses Asc as a reductant with much higher affinity for Asc than

436 plant-type VDE, in combination with a shift of its pH optimum towards lower values
437 enabling efficient de-epoxidation (Grouneva et al., 2006). Mosses have plant-type VDE
438 enzymes (Pinnola et al., 2013), which probably require Asc as a reductant. Since mosses
439 contain approx. ten times less Asc compared to vascular plants (Gest et al., 2013), it remains
440 to be explored how this low amount of Asc allows a rapid and intensive development of
441 NPQ, characteric of mosses (e.g. Marschall and Proctor, 2004).

442 In Chlamydomonas, light and O_2 availability-dependent state transition (qT),
443 involving major reorganizations of LHCs, also modulate NPQ (Depège, 2003; Lemeille et al.,
444 2009; Ünlü et al., 2014). Under our experimental conditions, ensuring aeration during both
445 the dark and the light adaptation, and using strong red light as actinic light, no decrease
446 occurred in the 685/710 nm ratio of the 77 K fluorescence spectra, suggesting that state I to
447 state II transition did not affect the NPQ induction in the wild type nor in the Asc-deficient
448 strains. The *stt7-9* mutant, unable to perform state transition, did not show decreased NPQ
449 (Supplemental Fig. S6), which would be expected if state transition would constitute a major
450 form of NPQ under our experimental conditions. However, our data do not exclude the
451 possibility that Asc may participate in state transition under conditions favoring its
452 occurrence.

453 A fourth, and rather complex component of NPQ is qI, possibly with several
454 underlying mechanisms involved (Adams et al., 2013; Tikkanen et al., 2014). We observed
455 both under photomixotrophic conditions at moderate light and under photoautotrophic
456 conditions that the slow NPQ component was enhanced in the *Crvtc2-1* mutant upon
457 illumination with strong red light, which, however, was not attributable to qZ or to qT.
458 Ascorbate deficiency is accompanied by an increase in the intracellular H_2O_2 content in
459 Chlamydomonas (Vidal-Meireles et al., 2017) and ROS are known to enhance NPQ via
460 several mechanisms (Roach and Na, 2017). Using H_2O_2 and catalase treatments (Fig. 5 and 8,

Supplemental Fig. S8), we clearly show that ROS formation is involved in the slowly induced NPQ component in the Asc-deficient strain that can be interpreted as qI. In the wild type, the contribution of qI to NPQ was probably minor under our experimental conditions, since catalase treatment did not diminish NPQ formation (Fig. 5D).

In conclusion, our results reveal fundamental differences between vascular plants and Chlamydomonas regarding the role of Asc in NPQ. Whereas in vascular plants, the most prominent role of Asc is to be a reductant of VDE, in Chlamydomonas, it is pertinent in preventing ROS formation that would lead to photoinhibitory quenching mechanisms.

Materials and Methods

Algal strains and growth conditions

Chlamydomonas reinhardtii strains CC-4533 (designated as wild type) and *LMJ.RY0402.058624* (designated as *Crvtc2-1*) were obtained from the CLiP library (Li et al., 2016b). The 137a (CC-125) strain and the *npq1* (CC-4100) mutant were obtained from the Chlamydomonas Resource Center (https://www.chlamycollection.org/). The *ARG7* complemented strain *cw15-412* (provided by Dr Michael Schroda (Technische Universität Kaiserslautern, Germany)) was used as control for the *stt7-9* mutant (Depège et al., 2003). The *VTC2*-amiRNA strain and its control *EV2* strain are described in Vidal-Meireles et al. (2017).

The synthetic coding sequence of *VTC2* including a 38 bp-long upstream sequence homologous to the *PSAD* 5'UTR with the BsmI restriction enzyme recognition site was ordered from Genecust (www.genecust.com). The *VTC2* insert was ligated as BsmI/EcoRI fragment into the similarily digested pJR39 (Neupert et al., 2009) vector, resulting in vector pJR112. Finally, pJR112 was digested with BsmI and SmaI and the *VTC2*-containing

BsmI/SmaI fragment was ligated to the similarily digested pJR91 vector that carries the *APH7''* resistance marker for selection on hygromycin-B. Transformation of the *Crvtc2-1* mutant strain was done via electroporation in a Bio-Rad GenePulser Xcell™ instrument, at 1000 V, with 10 F capacitance and infinite resistance usinga 4-mm gap cuvette. The cells were plated onto selective agar plates (TAP + 10 µg/ml hygromycin-B) and colonies were picked after 10 days of growth under moderate light (80 µmole photons m^{-2} s^{-1}).

Chlamydomonas pre-cultures were grown in 50-ml Erlenmeyer flasks in Tris-acetate phosphate (TAP) medium for three days at 22°C and 100 µmole photons m^{-2} s^{-1} on a rotatory shaker. Following this phase, cultures were grown in 100-ml Erlenmeyer flasks photomixotrophically (in TAP medium) or photoautotrophically (in high salt minimal (HSM) medium) at 22°C at 100 or 530 µmole photons m^{-2} s^{-1} for two additional days. The initial cell density was set to 1 million cells/ml.

DNA Isolation and PCR

Total genomic DNA from *C. reinhardtii* strains CC-4533 and *Crvt2-1* (*LMJ.RY0402.058624*) was extracted according to published protocols (Barahimipour et al., 2015; Schroda et al., 2001), and 1 µl of the extracted DNA were used as template for the PCR assays, using the GoTaq DNA polymerase (Promega GmbH).

To confirm the CIB1 insertion site in the *Crvt2-1* strain, PCR assays were conducted using gene specific primers that anneal upstream and downstream of the predicted insertion site of the cassette as well as primers specific for the 5' and 3' end of the CIB cassette. Primers 1 (5′-TGATGGCCAAGGGCTTAGTG-3′) and 2 (5'-CCGCAAACACCATGCAATCT-3′) amplified the region of the gene upstream the predicted site of CIB1 cassette insertion (control amplicon with an expected size of 852 bp), primers 3 (5′-AGATTGCATGGTGTTTGCGG-3′) and 4 (5′-CAGGCCATGTGAGAGTTTGCC-3′)

amplified the 3' junction site of the CIB1 cassette (amplicon with an expected size of 470 bp), and primers 5 (5′-GCACCAATCATGTCAAGCCT-3′) and 6 (5′-TGTTGTAGCCCACGCGGAAG-3′) amplified the 5' junction site of the cassette (amplicon with an expected size of 601 bp). The primers 11 (5′-GCTCTTGACTCGTTGTGCATTCTAG-3′) and 12 (5'-CACTGAGACACGTCGTACCTG -3′) amplified the 3' junction site of the *PsaD* promoter with the *VTC2* gene in the plasmid used for complementation (amplicon with an expected size of 841 bp).

Analyses of gene expression by qRT-PCR

Sample collection and RNA isolation was performed as in Vidal-Meireles et al., (2017). The primer pairs for the *VTC2* gene and the reference genes (*bTub2* - Cre12.g549550, *actin* - Cre13.g603700, *UBQ* - XP_001694320) used in real time qRT-PCR were published earlier in Vidal-Meireles et al. (2017). The annealing sites of the primers for analyzing *VTC2* expression are indicated as primers 7 and 8 in Fig. 1. Primers 9 (5′-AACCACCTGCACTTCCACGCTTAC-3′) and 10 (5'-TGCCCCGCAATCTCAAACGATG-3′) spanned the sequence encoding the catalytic site of *VTC2* (amplicon with an expected size of 434 bp).

The real time qRT-PCR data are presented as fold-change in mRNA transcript abundance of the *VTC2* gene, normalized to the average of the three reference genes, and relative to the untreated CC-4533 strain. Real-time qRT-PCR analysis was carried out with three technical replicates for each sample and three biological replicates were measured; the standard error was calculated based on the range of fold-change by calculating the minimum and the maximum of the fold-change using the standard deviations of ΔΔCt.

Determination of cell size, cell density, chlorophyll, Asc and carotenoid contents

536 The cell density was determined by a Scepter^{TM} 2.0 hand-held cell counter (Millipore), as
537 described in Vidal-Meireles et al., (2017).

538 The Chl content was determined according to Porra (1989) and the Asc content was
539 determined as in Kovács et al., (2016).

540 For carotenoid content determination, liquid culture containing 30 µg Chl(a+b)/ml
541 was filtered onto a Whatman glass microfibre filter (GF/C) and frozen in liquid N_2 at
542 different time points in the NPQ induction protocol. The pigments were extracted by re-
543 suspending the cells in 500 µl of ice-cold acetone. After re-suspension, the samples were
544 incubated in the dark for 30 min. This was followed by centrifugation at 11500 g, 4ºC, for 10
545 min and the supernatant was collected and passed through a PTFE 0.2 µm pore size syringe
546 filter.

547 Quantification of carotenoids was performed by HPLC using a Shimadzu Prominence
548 HPLC system (Shimadzu, Kyoto, Japan) consisting of two LC-20AD pumps, a DGU-20A
549 degasser, a SIL-20AC automatic sample injector, CTO-20AC column thermostat and a
550 Nexera X2 SPD-M30A photodiode-array detector. Chromatographic separations were carried
551 out on a Phenomenex Synergi Hydro-RP 250 x 4.6 mm column with a particle size of 4 µm
552 and a pore size of 80 Å. 20 µl aliquots of acetonic extract was injected to the column and the
553 pigments were eluted by a linear gradient from solvent A (acetonitrile, water, triethylamine,
554 in a ratio of 9:1:0.01) to solvent B (ethylacetate). The gradient from solvent A to solvent B
555 was run from 0 to 25 min at a flow rate of 1 ml/min. The column temperature was set to 25
556 °C. Eluates were monitored in a wavelength range of 260 nm to 750 nm at a sampling
557 frequency of 1.5625 Hz. Pigments were identified according to their retention time and
558 absorption spectrum and quantified by integrated chromatographic peak area recorded at the
559 wavelength of maximum absorbance for each kind of pigments using the corresponding
560 molar decadic absorption coefficient (Jeffrey et al., 1997). The de-epoxidation index of the

xanthophyll cycle components was calculated as (zeaxanthin + antheraxanthim)/(violaxanthin + anteraxanthin + zeaxanthin).

Chemical treatments

For Asc supplementation, 1 mM Na-Asc (Roth GmbH) was added to the cultures, and measurements were carried out after a 2 h incubation period in the light.

For H_2O_2 treatments, the cell density was adjusted to 3 million cells/ml and 1.5 mM H_2O_2 (Sigma Aldrich) was added. The presented measurements were carried out 7 h following the addition of H_2O_2.

Catalase (5 µg/ml, from bovine liver, Sigma Aldrich) was added after a 30-min dark adaptation and the measurements were carried out after an additional 2 h incubation period in the dark with shaking.

Western blot analysis

Protein isolation and western blot analysis were performed as in Vidal-Meireles et al., (2017). Specific polyclonal antibodies (produced in rabbits) against PsaA, PsbA, RbcL, LHCSR3, CP43, and PetB were purchased from Agrisera AB. Specific polyclonal antibody (produced in rabbits) against PSBO was purchased from AntiProt.

NPQ measurements

Chlorophyll *a* fluorescence was measured using a Dual-PAM-100 instrument (Heinz Walz GmbH, Germany). *C. reinhardtii* cultures were dark-adapted for 30 min and then liquid culture containing 30 µg Chl(a+b)/ml was filtered onto Whatman glass microfibre filters (GF/B) that was placed in between two microscopy cover slips with a spacer to allow for gas exchange. For NPQ induction, light adaptation consisted of 30 min illumination at 530 µmole

586 photons m^{-2} s^{-1}, followed by 12 min of dark adaptation interrupted with saturating pulses of
587 3000 µmole photons m^{-2} s^{-1}.
588
589 *Low-temperature fluorescence emission spectra (77K) measurements*
590 Algal cultures containing 2 µg Chl(a+b)/ml were collected at several time points during the
591 NPQ induction protocol. Subsequently, the sample was filtered onto a Whatman glass
592 microfibre filter (GF/C), placed in a sample holder and immediately frozen in liquid N_2. Low-
593 temperature (77K) fluorescence emission spectra were measured using a spectrofluorometer
594 (Fluorolog- 3/Jobin–Yvon–Spex Instrument S.A., Inc.) equipped with a home-made liquid
595 nitrogen cryostat. The fluorescence emission spectra between 650 and 750 nm were recorded
596 with an interval of 0.5 nm, using an excitation wavelength of 436 nm and excitation and
597 emission slits of 5 and 2 nm, respectively. The final spectra were corrected for the
598 photomultiplier's spectral sensitivity.
599
600 *Statistics*
601 The presented data are based on at least three independent experiments. When applicable,
602 averages and standard errors (±SE) were calculated. Statistical significance was determined
603 using one-way ANOVA followed by Dunnett multiple comparison post-tests (GraphPad
604 Prism 7.04; GraphPad Software, USA). Changes were considered statistically significant at p
605 < 0.05.
606
607 **Acknowledgements:**
608 The authors thank Prof. Dr. Ralph Bock (MPI-MP Potsdam, Germany) and Dr. Petar
609 Lambrev (BRC Szeged, Hungary) for discussions, Dr. Anikó Galambos (BRC Szeged,

610 Hungary) for the assistance with ordering the mutants from the CLiP library, and for Dr.
611 László Szabados (BRC Szeged, Hungary) for the possibility to use their CCD camera.

612

613 No conflicts of interest declared.

614 **References**

615 Adams WW III, Muller O, Cohu CM, Demmig-Adams B (2013) May photoinhibition be a
616 consequence, rather than a cause, of limited plant productivity? Photosynth Res 117:31-
617 44

618 Allorent G, Tokutsu R, Roach T, Peers G, Cardol P, Girard-Bascou J, Seigneurin-Berny D,
619 Petroutsos D, Kuntz M, Breyton C, Franck F, Wollman FA, Niyogi KK, Krieger-
620 Liszkay A, Minagawa J, Finazzi G (2013) A dual strategy to cope with high light in
621 *Chlamydomonas reinhardtii*. Plant Cell 25:545-557

622 Anwaruzzaman M, Chin BL, Li X-P, Lohr M, Martinez DA, Niyogi KK (2004) Genomic
623 analysis of mutants affecting xanthophyll biosynthesis and regulation of photosynthetic
624 light harvesting in Chlamydomonas reinhardtii. Photosynth Res 82:265-276

625 Arnoux P, Morosinotto T, Saga G, Bassi R, Pignol D (2009) A structural basis for the pH-
626 dependent xanthophyll cycle in *Arabidopsis thaliana*. Plant Cell 21: 2036-2044

627 Asada K (2006) Production and scavenging of reactive oxygen species in chloroplasts and
628 their functions. Plant Physiol 141: 391-396

629 Avenson TJ, Ahn TK, Zigmantas D, Niyogi KK, Li Z, Ballottari M, Bassi R, Fleming GR
630 (2008) Zeaxanthin radical cation formation in minor light-harvesting complexes of
631 higher plant antenna. J Biol Chem 283:3550-3558

632 Azzabi G, Pinnola A, Betterle N, Bassi R, Alboresi A (2012) Enhancement of non-photo de-
633 epoxidation index chemical quenching in the bryophyte *Physcomitrella patens* during
634 acclimation to salt and osmotic stress. Plant Cell Physiol 53: 1815-1825

635 Barahimipour R, Strenkert D, Neupert J, Schroda M, Merchant SS, Bock R (2015) Dissecting
636 the contributions of GC content and codon usage to gene expression in the model alga
637 *Chlamydomonas reinhardtii.* Plant J 84: 704-717

638 Baroli I, Do AD, Yamane T, Niyogi KK (2003) Zeaxanthin accumulation in the absence of a
639 functional xanthophyll cycle protects *Chlamydomonas reinhardtii* from photooxidative
640 stress. Plant Cell 15: 992-1008
641 Bratt C, Arvidsson P, Carlsson M, Akerlund H (1995) Regulation of violaxanthin de-
642 epoxidase activity by pH and ascorbate. Photosynth Res 45: 169-175
643 Bonente G, Ballottari M, Truong T, Morosinotto T, Ahn T, Fleming G, Niyogi K, Bassi R
644 (2011) Analysis of LhcSR3, a protein essential for feedback de- excitation in the green
645 alga *Chlamydomonas reinhardtii*. PLoS Biol 9:e1000577
646 Bradbury LMT, Shumskaya M, Tzfadia O, Wu S-B, Kennelly EK, Wurtzelt ET (2012)
647 Lycopene cyclase paralog CruP protects against reactive oxygen species in oxygenic
648 photosynthetic organisms. Proc Natl Acad Sci USA 109:E1888-E1897
649 Chaux F, Johnson X, Auroy P, Beyly-Adriano A, Te I, Cuiné S, Peltier G (2017) PGRL1 and
650 LHCSR3 compensate for each other in controlling photosynthesis and avoiding
651 photosystem I photoinhibition during high light acclimation of Chlamydomonas cells.
652 Mol Plant 10:216-218
653 Christa G, Cruz S, Jahns P, de Vries J, Cartaxana P, Esteves AC, Serôdio J, Gould SB (2017)
654 Photoprotection in a monophyletic branch of chlorophyte algae is independent of
655 energy-dependent quenching (qE). New Phytol 214: 1132-1144
656 Depège N, Bellafiore S, Rochaix JD (2003) Role of chloroplast protein kinase Stt7 in LHCII
657 phosphorylation and state transition in Chlamydomonas. Science 299: 1572-1575
658 Dowdle J, Ishikawa T, Gatzek S, Rolinski S, Smirnoff N (2007) Two genes in *Arabidopsis*
659 *thaliana* encoding GDP-L-galactose phosphorylase are required for ascorbate
660 biosynthesis and seedling viability. Plant J 52: 673-689
661 Erickson E, Wakao S, Niyogi KK (2015) Light stress and photoprotection in *Chlamydomonas*
662 *reinhardtii.* Plant J 82:449-465

663 Fernie AR, Tóth SZ (2015) Identification of the elusive chloroplast ascorbate transporter
664 extends the substrate specificity of the PHT family. Mol Plant 8:674-676
665 Finazzi G, Johnson GN, Dall'Osto L, Zito F, Bonente G, Bassi R, Wollman F-A (2006)
666 Nonphotochemical quenching of chlorophyll fluorescence in *Chlamydomonas*
667 *reinhardtii*. Biochemistry 45:1490-1498
668 Foyer CH, Shigeoka S (2011) Understanding oxidative stress and antioxidant functions to
669 enhance photosynthesis. Plant Physiol 155: 93-100
670 Gest N, Gautier H, Stevens R (2013) Ascorbate as seen through plant evolution: the rise of a
671 successful molecule? J Exp Bot 64:33-53
672 Grouneva I, Jakob T, Wilhelm C, Goss R (2006) Influence of ascorbate and pH on the
673 activity of the diatom xanthophyll cycle-enzyme diadinoxanthin de-epoxidase. Physiol
674 Plant 126:205-211
675 Hager A, Holocher K (1994) Localization of the xanthophyll-cycle enzyme violaxanthin de-
676 epoxidase within the thylakoid lumen and abolition of its mobility by a (light-
677 dependent) pH decrease. Planta 192: 581-589
678 Hallin EI, Hasan M, Guo K, Åkerlund H-E (2016) Molecular studies on structural changes
679 and oligomerisation of violaxanthin de-epoxidase associated with the pH-dependent
680 activation. Photosynth Res 129: 29-41
681 Hieber AD, Bugos RC, Yamamoto HY (2000) Plant lipocalins: violaxanthin de-epoxidase
682 and zeaxanthin epoxidase. Biochim Biophys Acta BBA - Protein Struct Mol Enzymol
683 1482: 84-91
684 Holt NE, Zigmantas D, Valkunas L, Li X-P, Niyogi KK, Fleming GR (2005) Carotenoid
685 cation formation and the regulation of photosynthetic light harvesting. Science
686 307:433-436

687 Holub O, Seufferheld MJ, Gohlke C, Heiss GJ, Clegg RM (2007) Fluorescence lifetime
688 imaging microscopy of *Chlamydomonas reinhardtii*: non-photochemical quenching
689 mutants and the effect of photosynthetic inhibitors on the slow chlorophyll fluorescence
690 transient. J Microsc 226: 90-120
691 Ivanov B, Asada K, Edwards GE (2007) Analysis of donors of electrons to photosystem I and
692 cyclic electron flow by redox kinetics of P700 in chloroplasts of isolated bundle sheath
693 strands of maize. Photosynth Res 92:65-74
694 Iwai M, Kato N, Minagawa J (2007) Distinct physiological responses to a high light and low
695 CO_2 environment revealed by fluorescence quenching in photoautotrophically grown
696 *Chlamydomonas reinhardtii*. Photosynth Res 94:307-314
697 Jeffrey SW, Mantoura RFC, Wright SW (1997) Phytoplankton pigments in oceanography:
698 guidelines to modern methods. (Paris: UNESCO Publishing)
699 Johnson X, Alric J (2012) Interaction between starch breakdown, acetate assimilation, and
700 photosynthetic cyclic electron flow in *Chlamydomonas reinhardtii*. J Biol Chem
701 287:26445-26452
702 Johnson MP, Davison PA, Ruban AV, Horton P (2008) The xanthophyll cycle pool size
703 controls the kinetics of non-photochemical quenching in *Arabidopsis thaliana*. FEBS
704 Lett 582:259-263
705 Kanazawa A, Kramer DM (2002). In vivo modulation of nonphotochemical exciton
706 quenching (NPQ) by regulation of the chloroplast ATP synthase. Proc Natl Acad Sci
707 USA 99:12789-12794
708 Kovács L, Vidal-Meireles A, Nagy V, Tóth SZ (2016) Quantitative determination of
709 ascorbate from the green alga *Chlamydomonas reinhardtii* by HPLC. Bio-Protoc
710 6:e2067

711 Lemeille S, Willig A, Depège-Fargeix N, Delessert C, Bassi R, Rochaix J-D (2009) Analysis
712 of the chloroplast protein kinase Stt7 during state transitions. PLoS Biol 7: e1000045
713 Li S, Liu L, Zhuang X, Yu Y, Liu X, Cui X, Ji L, Pan Z, Cao X, Mo B, Zhang F, Raikhel N,
714 Jiang L, and Chen X (2013) MicroRNAs inhibit the Ttranslation of target mRNAs on
715 the endoplasmic reticulum in Arabidopsis. Cell 153: 562-574
716 Li Z, Peers G, Dent RM, Bai Y, Yang SY, Apel W, Leonelli L, Niyogi KK (2016a) Evolution
717 of an atypical de-epoxidase for photoprotection in the green lineage. Nat Plants 2:
718 16140
719 Li X, Zhang R, Patena W, Gang SS, Blum SR, Ivanova N, Yue R, Robertson JM, Lefebvre
720 PA, Fitz-Gibbon ST, Grossman AR, Jonikas MC (2016b) An indexed, mapped mutant
721 library enables reverse genetics studies of biological processes in *Chlamydomonas*
722 *reinhardtii*. Plant Cell 28: 367-387
723 Marschall M, Proctor MCF (2004) Are bryophytes shade plants? Photosynthetic light
724 responses and proportions of chlorophyll *a*, chlorophyll b and total carotenoids. Ann
725 Bot 94: 593-603
726 Müller-Moulé P, Conklin PL, Niyogi KK (2002) Ascorbate deficiency can limit violaxanthin
727 de-epoxidase activity in vivo. Plant Physiol 128: 970-977
728 Müller-Moulé P, Havaux M, Niyogi KK (2003) Zeaxanthin deficiency enhances the high
729 light sensitivity of an ascorbate-deficient mutant of Arabidopsis. Plant Physiol 133:
730 748-760.
731 Nagy V, Vidal-Meireles A, Podmaniczki A, Szentmihályi K, Rákhely G, Zsigmond L,
732 Kovács L, Tóth SZ (2018) The mechanism of photosystem II inactivation during
733 sulphur deprivation-induced H_2 production in *Chlamydomonas reinhardtii*. Plant J
734 94:548-561

735 Neupert J, Karcher D, Bock R (2009) Generation of Chlamydomonas strains that efficiently
736 express nuclear transgenes. Plant J 57:1140-1150
737 Niyogi KK, Bjorkman O, Grossmann AR (1997) Chlamydomonas xanthophyll cycle mutants
738 identified by video imaging of chlorophyll fluorescence quenching. Plant Cell 9:1369-
739 1380
740 Peers G, Truong TB, Ostendorf E, Busch A, Elrad D, Grossman AR, Hippler M, Niyogi KK
741 (2009) An ancient light-harvesting protein is critical for the regulation of algal
742 photosynthesis. Nature 462:518-521
743 Pinnola A, Dall'Osto L, Gerotto C, Morosinotto T, Bassi R, Alboresi A (2013) Zeaxanthin
744 binds to Light-Harvesting Complex Stress-Related Protein to enhance
745 nonphotochemical quenching in *Physcomitrella patens*. Plant Cell 25:3519-3534
746 Polukhina I, Fristedt R, Dinc E, Cardol P, Croce R (2016) Carbon supply and
747 photoacclimation cross talk in the green alga *Chlamydomonas reinhardtii*. Plant Physiol
748 172: 1494-1505
749 Porra RJ, Thompson WA, Kriedeman PE (1989) Determination of accurate extinction
750 coefficients and simultaneous equations for essaying chlorophylls-a and -b with four
751 different solvents: verification of the concentration of chlorophyll standards by atomic
752 absorption spectroscopy. Biochim Biophys Acta 975: 384-394
753 Quaas T, Berteotti S, Ballottari M, Flieger K, Bassi R, Wilhelm C, Goss R (2015) Non-
754 photochemical quenching and xanthophyll cycle activities in six green algal species
755 suggest mechanistic differences in the process of excess energy dissipation. J. Plant
756 Physiol 172: 92-103
757 Roach T, Na CS (2017) LHCSR3 affects de-coupling and re-coupling of LHCII to PSII
758 during state transitions in *Chlamydomonas reinhardtii*. Sci Rep 7: 43145

759 Ruban AV, Johnson MP, Duffy CD (2012) The photoprotective molecular switch in the
760 photosystem II antenna. Biochim Biophys Acta 1817:167-181
761 Saga G, Giorgetti A, Fufezan C, Giacometti GM, Bassi R, Morosinotto T (2010) Mutation
762 analysis of violaxanthin de-epoxidase identifies substrate-binding sites and residues
763 involved in catalysis. J Biol Chem 285:23763-23770
764 Schroda M, Vallon O, Whitelegge JP, Beck CF, Wollman FA (2001) The chloroplastic GrpE
765 homolog of Chlamydomonas: two isoforms generated by differential splicing. Plant
766 Cell 13:2823-2839
767 Smirnoff N (2018) Ascorbic acid metabolism and functions: A comparison of plants and
768 mammals. Free Radic Biol Med. 122:116-129
769 Takizawa K, Kanazawa A, Kramer DM (2008) Depletion of stromal Pi induces high 'energy
770 dependent' antenna exciton quenching (qE) by decreasing proton conductivity at CFO-
771 CF1 ATP synthase. Plant Cell Environ 31:235-243
772 Tibiletti T, Auroy P, Peltier G, Caffarri S (2016) *Chlamydomonas reinhardtii* PsbS protein is
773 functional and accumulates rapidly and transiently under high light. Plant Physiol
774 171:2717-2730
775 Tikkanen M, Mekala NR, Aro E-M (2014) Photosystem II photoinhibition-repair cycle
776 protects photosystem I from irreversible damage. Biochim Biophys Acta - Bioenerg
777 1837: 210-215
778 Tóth SZ, Puthur JT, Nagy V, Garab G (2009) Experimental evidence for ascorbate-dependent
779 electron transport in leaves with inactive oxygen-evolving complexes. Plant Physiol
780 149: 1568-1578
781 Tóth SZ, Nagy V, Puthur JT, Kovács L, Garab G (2011) The physiological role of ascorbate
782 as photosystem II electron donor: Protection against photoinactivation in heat-stressed
783 leaves. Plant Physiol 156: 382-392

784 Tóth SZ, Lőrincz T, Szarka A (2018) Concentration does matter: The beneficial and
785 potentially harmful effects of ascorbate in humans and plants. Antioxid Redox Signal
786 29:1516-1533
787 Ünlü C, Drop B, Croce R, van Amerongen H (2014) State transitions in *Chlamydomonas*
788 *reinhardtii* strongly modulate the functional size of photosystem II but not of
789 photosystem I. Proc Natl Acad Sci USA 111:3460-3465
790 Urzica EI, Adler LN, Page MD, Linster CL, Arbing MA, Casero D, Pellegrini M, Merchant
791 SS, Clarke SG (2012) Impact of oxidative stress on ascorbate biosynthesis in
792 Chlamydomonas via regulation of the *VTC2* gene encoding a GDP-L-galactose
793 phosphorylase. J Biol Chem 287: 14234-14245
794 Vidal-Meireles A, Neupert J, Zsigmond L, Rosado-Souza L, Kovács L, Nagy V, Galambos
795 A, Fernie AR, Bock R, Tóth SZ (2017) Regulation of ascorbate biosynthesis in green
796 algae has evolved to enable rapid stress-induced response via the *VTC2* gene encoding
797 GDP- L -galactose phosphorylase. New Phytol 214: 668-681
798 Voigt J, Münzner P (1994) Blue light-induced lethality of a cell wall-deficient mutant of the
799 unicellular green alga *Chlamydomonas reinhardtii*. Plant Cell Physiol 35: 99-106
800 Wang Z, Xiao Y, Chen W, Tang K, Zhang L (2010) Increased vitamin C content
801 accompanied by an enhanced recycling pathway confers oxidative stress tolerance in
802 Arabidopsis. J. Integr. Plant Biol 52: 400-409
803 Wheeler G, Ishikawa T, Pornsaksit V, Smirnoff N (2015) Evolution of alternative
804 biosynthetic pathways for vitamin C following plastid acquisition in photosynthetic
805 eukaryotes. eLife 4:e06369
806 Xue H, Tokutsu R, Bergner SV, Scholz M, Minagawa J, Hippler M (2015) Photosystem II
807 subunit R is required for efficient binding of Light-Harvesting Complex Stress-Related

Protein 3 to photosystem II-light-harvesting supercomplexes in *Chlamydomonas reinhardtii*. Plant Physiol 167: 1566-1578

Zechmann B, Stumpe M, Mauch F (2011) Immunocytochemical determination of the subcellular distribution of ascorbate in plants. Planta 233: 1-12

812 **Figure legends**

813

814 **Figure 1.** Characterization of an insertional CLiP mutant of *C. reinhardtii*
815 (*LMJ.RY0402.058624*, named *Crvtc2-1*), affected in the *VTC2* gene that encodes GDP-L-
816 galactose phosphorylase. A, Physical map of the *VTC2* gene (obtained from Phytozome
817 v12.1.6) with the CIB1 cassette insertion site in the *Crvtc2-1* mutant. Exons are shown in
818 black, introns in light grey, and promoter/ 5' UTR and terminator sequences in dark grey.
819 Insertion site of the CIB1 cassette is indicated by triangle and the binding sites of the primers
820 used for genotyping and gene expression analysis of *Crvtc2-1* are shown as black arrows. The
821 sequence encoding the catalytic site of GDP-L-galactose phosphorylase is marked as a white
822 line within Exon 3; B, PCR performed using primers annealing upstream the predicted
823 cassette insertion site in *VTC2* (top panel, using primers P1+P2), and using primers
824 amplifying the 5' and 3' genome-cassette junctions (using primers P3+P4 and P5+P6,
825 respectively, middle and bottom panels). The expected sizes are marked with arrows; C,
826 Ascorbate contents of the wild type (CC-4533) and the *Crvtc2-1* mutant grown
827 mixotrophically in TAP medium at moderate light with and without the addition of 1.5 mM
828 H_2O_2; D, Transcript levels of *VTC2*, as determined by real-time qRT-PCR in cultures
829 supplemented or not with H_2O_2, using primers P7+P8. E, qRT-PCR analysis using primers
830 P9+P10, spanning the sequence that encodes the catalytic site of GDP-L-galactose
831 phosphorylase. The number of PCR cycles is indicated at the bottom of the figure. Data was
832 analyzed by one-way ANOVA followed by Dunnett post-test: × $p<0.05$, ×× $p<0.01$, ×××× $p<0.0001$ compared to the untreated CC-4533 strain.

834

835 **Figure 2.** Complementation of the insertional CLiP mutant *LMJ.RY0402.058624*, affected in
836 the *VTC2* gene (named *Crvtc2-1*) with the coding sequence of *VTC2*. A, Physical map of the

837 *Crvtc2-1+VTC2* plasmid containing the coding sequence of *VTC2*, the constitutive promoter
838 *PsaD* and the *APH7"* resistance gene. Exons are shown in black and promoter/ 5' UTR,
839 terminator sequences in dark grey, and the sequence encoding the catalytic site of GDP-L-
840 galactose phosphorylase is marked as a white line. The binding sites of the primers used
841 below are shown as black arrows; B, PCR performed using primers annealing in the promoter
842 and *VTC2* exon 1 (P11+P12). The expected size is marked with an arrow; C, qRT-PCR
843 performed using primers annealing to the sequence encoding the catalytic site of *VTC2*
844 (P9+P10). The expected size is marked with an arrow; D, Ascorbate contents of CC-4533, the
845 *Crvtc2-1* mutant and the complementation lines *Crvtc2-1+VTC2* grown for 3 days in TAP at
846 100 µmole photons m^{-2} s^{-1}. Data was analyzed by one-way ANOVA followed by Dunnett
847 post-test: × $p<0.05$, ××× $p<0.001$, ×××× $p<0.0001$ compared to the CC-4533 strain. µE
848 stands for µmole photons m^{-2} s^{-1}.
849
850 **Figure 3.** Acclimation to 530 µmole photons m^{-2} s^{-1} of red light followed by recovery in CC-
851 4533 (wild type) and *Crvtc2-1* cultures, grown photomixotrophically in TAP medium at 100
852 µmole photons m^{-2} s^{-1}. A, NPQ kinetics; B, De-epoxidation index; C, F_V/F_M parameter
853 measured after dark adaptation and after recovery from the 530 µmole photons m^{-2} s^{-1} red
854 light; D, 684 nm/ 710 nm ratio of the 77K fluorescence spectra. Samples were collected at the
855 growth light of 100 µmole photons m^{-2} s^{-1}, after 30 min of dark-adaptation, at the end of the
856 30 min light period to 530 µmole photons m^{-2} s^{-1} and 15 min after the cessation of actinic
857 illumination, as indicated by arrows in the scheme in panel A. Data was analyzed by one-way
858 ANOVA followed by Dunnett post-test: ## $p<0.01$ compared to the CC-4533 strain at the
859 respective time-point; × $p<0.05$, ×× $p<0.01$, ××× $p<0.001$ compared to the dark-adapted CC-
860 4533 strain. µE stands for µmole photons m^{-2} s^{-1}.
861

862 **Figure 4.** Effects of overnight (16 h) dark acclimation on the CC-4533 and the *Crvtc2-1*
863 (grown in TAP medium at 100 µmole photons m^{-2} s^{-1}). A, Ascorbate content after 16 h of
864 dark acclimation; B, NPQ, induced by 530 µmole photons m^{-2} s^{-1} of red light after overnight
865 dark acclimation; C, de-epoxidation index, determined in the overnight dark-acclimated
866 cultures, after strong red-light illumination and following recovery. Data was analyzed by
867 one-way ANOVA followed by Dunnett post-test: ××× $p<0.001$, ×××× $p<0.0001$ compared to
868 the dark-acclimated CC-4533 strain. µE stands for µmole photons m^{-2} s^{-1}.
869
870 **Figure 5.** The effects of H_2O_2 and catalase on NPQ, induced by strong red light (530 µmole
871 photons m^{-2} s^{-1}) in the wild type (CC-4533) and the *Crvtc2-1* mutant grown in
872 photomixotrophic conditions in TAP medium at 100 µmole photons m^{-2} s^{-1}. A, The effect of
873 1.5 mM H_2O_2 on NPQ induction in the CC-4533 strain; B, the effect of 1.5 mM H_2O_2 on
874 NPQ induction in the *Crvtc2-1* mutant; C, the effect of H_2O_2 addition on de-epoxidation; D,
875 the effect of catalase on NPQ induction in the CC-4533 strain; E, the effect of catalase on
876 NPQ induction in the *Crvtc2-1* mutant. Samples were collected at the time points indicated
877 by arrows in the schemes in panels A and B. Data was analyzed by one-way ANOVA
878 followed by Dunnett post-test: ## $p<0.01$, ### $p<0.001$, #### $p<0.0001$ compared to the
879 untreated CC-4533 culture at the respective time-point; × $p<0.05$, ×× $p<0.01$, ××× $p<0.001$
880 compared to the dark-adapted CC-4533 strain. µE stands for µmole photons m^{-2} s^{-1}.
881
882 **Figure 6.** Effects of strong red light (530 µmole photons m^{-2} s^{-1}) on the 137a (wild type) and
883 the *npq1* mutant of *C. reinhardtii* grown in TAP medium at 100 µmole photons m^{-2} s^{-1}. A,
884 NPQ induced by 530 µmole photons m^{-2} s^{-1} of red light followed by a recovery phase; B,
885 F_V/F_M value, determined before the strong red light illumination and after the recovery phase;
886 C, Chl(a+b) content of the cultures determined before, during and after the strong red light

887 illumination; D, β-carotene content measured before, during and after the strong red light
888 illumination; E, 684 nm/ 710 nm ratio of the 77K fluorescence spectra determined before,
889 during and after the strong red light illumination; F, Ascorbate contents of the *npq1* and
890 *Crvtc2-1* mutants and the CC-4533 and 137a wild type strains. Samples were collected at the
891 time points indicated by arrows in the scheme in panel A. Data was analyzed by one-way
892 ANOVA followed by Dunnett post-test: #### $p<0.0001$ compared to the 137a strain at the
893 respective time-point; + $p<0.05$, ++ $p<0.01$, ++++ $p<0.0001$ compared to the dark-adapted
894 137a strain; ×× $p<0.01$, ×××× $p<0.0001$ compared to the CC-4533 strain. µE stands for
895 µmole photons m^{-2} s^{-1}.
896
897 **Figure 7.** Acclimation to 530 µmole photons m^{-2} s^{-1} of red light followed by recovery in CC-
898 4533 and *Crvtc2-1* cultures, grown photoautotrophically in HSM medium at 530 µmole
899 photons m^{-2} s^{-1}. A, NPQ kinetics; B, De-epoxidation index; C, F_V/F_M parameter measured
900 after dark adaptation and after recovery from the 530 µmole photons m^{-2} s^{-1} red light
901 illumination; D, 684 nm/ 710 nm ratio of the 77K fluorescence spectra. The samples were
902 collected at the growth light of 530 µmole photons m^{-2} s^{-1}, after 30 min of dark adaptation, at
903 the end of the 30 min red light illumination, and 12 min after the cessation of actinic
904 illumination, as indicated in the scheme in panel A. Data was analyzed by one-way ANOVA
905 followed by Dunnett post-test: #### $p<0.0001$ compared to the CC-4533 strain at the
906 respective time-point; × $p<0.05$, ×× $p<0.01$, ××× $p<0.001$ compared to the dark-adapted CC-
907 4533 strain. µE stands for µmole photons m^{-2} s^{-1}.
908
909 **Figure 8.** The effects of H_2O_2 and catalase on NPQ induced by strong red light (530 µmole
910 photons m^{-2} s^{-1}) in the wild type (CC-4533) and *Crvtc2-1* mutant strains grown
911 photoautotrophically in HSM medium at 530 µmole photons m^{-2} s^{-1}. A, The effect of 1.5 mM

912 H_2O_2 on NPQ induction in the CC-4533 strain; B, the effect of 1.5 mM H_2O_2 on NPQ
913 induction in the *Crvtc2-1* mutant; C, the effect of catalase on NPQ induction in the CC-4533
914 strain; D, the effect of catalase on NPQ induction in the *Crvtc2-1* mutant. Data was analyzed
915 by one-way ANOVA followed by Dunnett post-test: # $p<0.05$, #### $p<0.0001$ compared to
916 the untreated CC-4533 culture at the respective time-point. µE stands for µmole photons m^{-2}
917 s^{-1}.

Supplemental figures

Supplemental Fig. S1. Confirmation of the location of the CIB1 casette in the insertional CLiP mutant of *C. reinhardtii* (*LMJ.RY0402.058624*, named *Crvtc2-1*), affected in the *VTC2* gene. A, Physical map of the *VTC2* gene (obtained from Phytozome v12.1.6) with the CIB1 cassette insertion site in the *Crvtc2-1* mutant. Exons are shown in black, intron in light grey. Insertion site of the CIB1 cassette is indicated by triangle and the sequencing region is marked by arrows; B, Sequencing results using the Multiple Sequence Alignment by CLUSTALW (https://www.genome.jp/tools-bin/clustalw).

Supplemental Fig. S2. Characterization of the CC-4533 (wild-type), *Crvtc2-1* mutant, and *Crvtc2-1+VTC2* complemented *C. reinhardtii* lines. A, Cell volume. B, Chl(a+b) per million cells. C, Chl *a*/*b* ratio. D, Increase in Chl(a+b) concentration during culture growth in mixotrophic conditions (TAP) at moderate and high light (100 and 530 µmole photons m^{-2} s^{-1}, respectively) and in photoautotrophic conditions (HSM) at 530 µmole photons m^{-2} s^{-1}. E, Cellular Asc content after 24 h of growth under conditions corresponding to panel D. Data was analyzed by one-way ANOVA followed by Dunnett post-test: ××× $p<0.05$; ×× $p<0.01$; ××× $p<0.001$; ×××× $p<0.0001$ compared to the CC-4533 strain at the respective time-point and treatment. µE stands for µmole photons m^{-2} s^{-1}.

Supplemental Fig. S3. Western blot analysis for the semi-quantitative determination of PsbA, CP43, PSBO, PsaA, LHCSR3, PetB and RbcL contents in *C. reinhardtii* cultures grown under photomixotrophic conditions at moderate light (100 µmole photons m^{-2} s^{-1}) and photoautotrophic conditions at moderate and high light (100 and 530 µmole photons m^{-2} s^{-1} respectively). Samples of 1 µg Chl(a+b) were loaded, and the first four lanes (25, 50, 100,

and 200% of the CC-4553 strain grown under photomixotrophic conditions at 100 µmole photons m^{-2} s^{-1}) are for the approximate quantitation of the proteins. The graphics represent the densitometry analysis based on three independent experiments. Data was analyzed by one-way ANOVA followed by Dunnett post-test: ×<0.05, ××<0.01, ×××<0.001 compared to the TAP-grown CC-4533 culture. µE stands for µmole photons m^{-2} s^{-1}.

Supplemental Fig. S4. NPQ kinetics induced by strong red light (530 µmole photons m^{-2} s^{-1}) in cultures grown either in photomixotrophic conditions in TAP medium at 100 µmole photons m^{-2} s^{-1} or in photoautotrophic conditions in HSM medium at 530 µmole photons m^{-2} s^{-1}. A and B, NPQ kinetics of the CC-4533 (wild type), *Crvtc2-1* and *Crvtc2-1+VTC2* complemented lines; C and D, NPQ kinetics of the *VTC2-amiRNA* and empty vector (*EV2*) lines. Data was analyzed by one-way ANOVA followed by Dunnett post-test: #<0.05, ##<0.01 compared to the untreated CC-4533 culture at the respective time-point. µE stands for µmole photons m^{-2} s^{-1}.

Supplemental Fig. S5. Carotenoid contents of the *Crvtc2-1* mutant and the wild type (CC-4533) during NPQ induction by strong red light (530 µmole photons m^{-2} s^{-1}). The cultures were grown in photomixotrophic conditions in TAP medium at 100 µmole photons m^{-2} s^{-1}. A, Violaxanthin; B, antheraxanthin; C, zeaxanthin; D, β-carotene; E, lutein concentrations. Data was analyzed by one-way ANOVA followed by Dunnett post-test: × $p<0.05$, ×× $p<0.01$, ×××× $p<0.0001$ compared to the dark-adapted CC-4533 strain.

Supplemental Fig. S6. NPQ induction in the *stt7-9* mutant of *C. reinhardtii* and in *cw15-412*, used as a control strain, grown in TAP medium at 100 µmole photons m^{-2} s^{-1}. A, NPQ kinetics, induced by 530 µmole photons m^{-2} s^{-1} of red light and followed by a recovery phase;

968 B, de-epoxidation index, determined in the growth light, after 30 min of dark adaptation,
969 following illumination with strong red light, and after the recovery phase, as indicated in the
970 scheme in panel A. Data was analyzed by one-way ANOVA followed by Dunnett post-test:
971 #<0.05, ####<0.0001 compared to the *cw15-412* strain at the respective time-point; ××
972 p<0.01, ×××× p<0.0001 compared to the dark-adapted *cw15-412* strain. µE stands for µmole
973 photons m-2 s^{-1}.
974
975 **Supplemental Fig. S7.** Carotenoid contents of the *Crvtc2-1* mutant and the wild type (CC-
976 4533) during NPQ induction upon strong red light (530 µmole photons m^{-2} s^{-1}). The cultures
977 were grown in photoautotrophic conditions in HSM medium at 530 µmole photons m^{-2} s^{-1}. A,
978 Violaxanthin; B, antheraxanthin; C, zeaxanthin; D, β-carotene; E, lutein concentrations. Data
979 was analyzed by one-way ANOVA followed by Dunnett post-test: × p<0.05, ×× p<0.01, ×××
980 p<0.001, ×××× p<0.0001 compared to the dark-adapted CC-4533 strain.
981
982 **Supplemental Fig. S8.** Acclimation to 530 µmole photons m^{-2} s^{-1} of red light followed by
983 recovery in CC-4533 and *Crvtc2-1* cultures, grown photoautotrophically in HSM medium at
984 100 µmole photons m^{-2} s^{-1}. A, NPQ kinetics; B, De-epoxidation index; C, F_V/F_M parameter
985 measured after dark adaptation and after strong red light illumination. D, 684 nm/ 710 nm
986 ratio of the 77K fluorescence spectra. Samples were collected at the growth light of 100
987 µmole photons m^{-2} s^{-1}, after 30 min of dark-adaptation, at the end of the 30 min strong red
988 light illumination, and 12 min after the cessation of actinic illumination, as indicated by
989 arrows in the scheme in panel A. E, The effect of 1.5 mM H_2O_2 on NPQ induction in the CC-
990 4533 strain; F, the effect of 1.5 mM H_2O_2 on NPQ induction in the *Crvtc2-1* mutant; G, the
991 effect of catalase on NPQ induction in the CC-4533 strain; H, the effect of catalase on NPQ
992 induction in the *Crvtc2-1* mutant. Data was analyzed by one-way ANOVA followed by

993 Dunnett post-test: × $p<0.05$, ×× $p<0.01$, ×××× $p<0.0001$ compared to the dark-adapted CC-

994 4533 strain. µE stands for µmole photons m^{-2} s^{-1}.

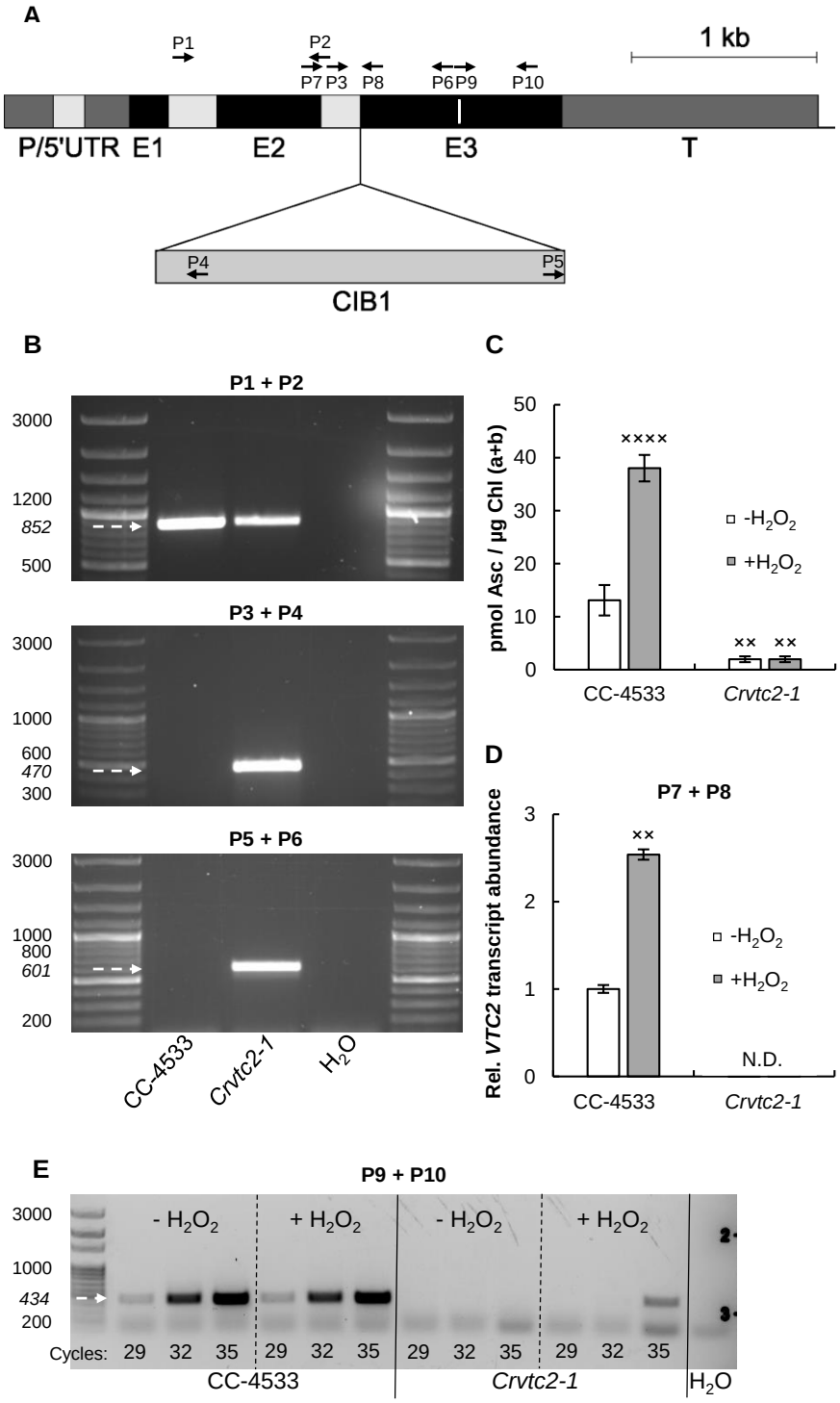

Figure 1. Characterization of an insertional CLiP mutant of *C. reinhardtii* (*LMJ.RY0402.058624*, named *Crvtc2-1*), affected in the VTC2 gene that encodes GDP-L-galactose phosphorylase. A, Physical map of the *VTC2* gene (obtained from Phytozome v12.1.6) with the CIB1 cassette insertion site in the *Crvtc2-1* mutant. Exons are shown in black, introns in light grey, and promoter/ 5' UTR and terminator sequences in dark grey. Insertion site of the CIB1 cassette is indicated by triangle and the binding sites of the primers used for genotyping and gene expression analysis of *Crvtc2-1* are shown as black arrows. The sequence encoding the catalytic site of GDP-L-galactose phosphorylase is marked as a white line within Exon 3; B, PCR performed using primers annealing upstream the predicted cassette insertion site in *VTC2* (top panel, using primers P1+P2), and using primers amplifying the 5' and 3' genome-cassette junctions (using primers P3+P4 and P5+P6, respectively, middle and bottom panels). The expected sizes are marked with arrows; C, Ascorbate contents of the wild type (CC-4533) and the *Crvtc2-1* mutant grown mixotrophically in TAP medium at moderate light with and without the addition of 1.5 mM H_2O_2; D, Transcript levels of *VTC2*, as determined by real-time qRT-PCR in cultures supplemented or not with H_2O_2, using primers P7+P8. E, qRT-PCR analysis using primers P9+P10, spanning the sequence that encodes the catalytic site of GDP-L-galactose phosphorylase. The number of PCR cycles is indicated at the bottom of the figure. Data was analyzed by one-way ANOVA followed by Dunnett post-test: × $p<0.05$, ×× $p<0.01$, ×××× $p<0.0001$ compared to the untreated CC-4533 strain.

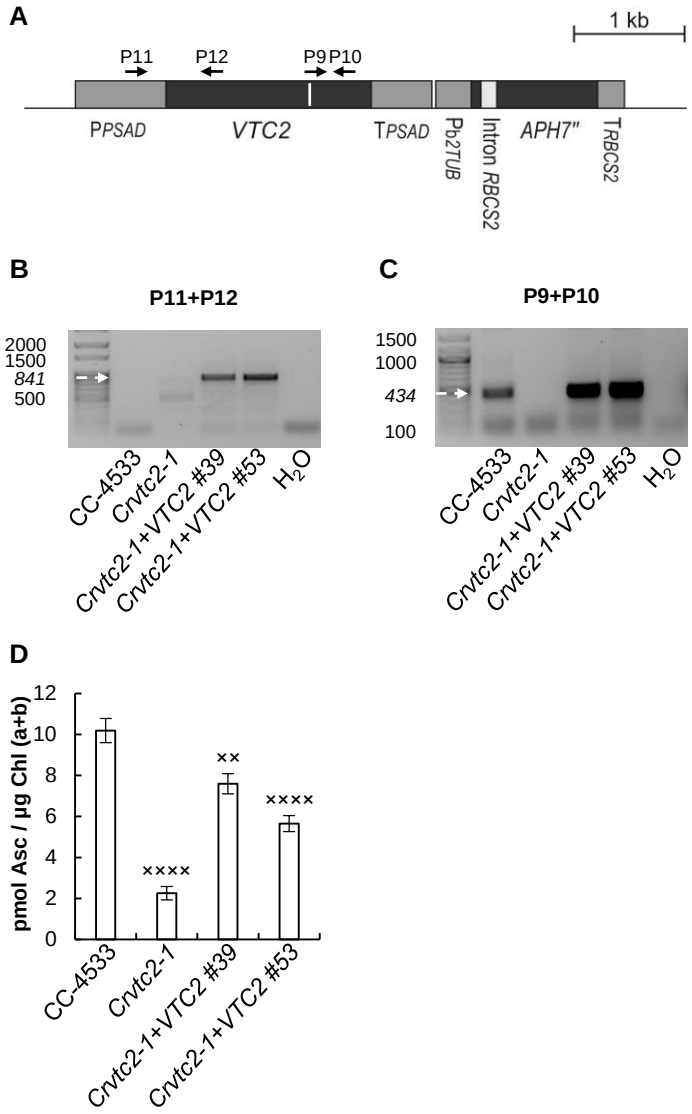

Figure 2 – Complementation of the insertional CLiP mutant *LMJ.RY0402.058624,* affected in the *VTC2* gene (named *Crvtc2-1*) with the coding sequence of *VTC2*. A, Physical map of the *Crvtc2-1+VTC2* plasmid containing the coding sequence of *VTC2*, the constitutive promoter *PsaD* and the *APH7"* resistance gene. Exons are shown in black and promoter/ 5' UTR, terminator sequences in dark grey, and the sequence encoding the catalytic site of GDP-L-galactose phosphorylase is marked as a white line. The binding sites of the primers used below are shown as black arrows; B, PCR performed using primers annealing in the promoter and *VTC2* exon 1 (P11+P12). The expected size is marked with an arrow; C, qRT-PCR performed using primers annealing to the sequence encoding the catalytic site of *VTC2* (P9+P10). The expected size is marked with an arrow; D, Ascorbate contents of CC-4533, the *Crvtc2-1* mutant and the complementation lines *Crvtc2-1+VTC2* grown for 3 days in TAP at 100 µmole photons m^{-2} s^{-1}. Data was analyzed by one-way ANOVA followed by Dunnett post-test: × $p<0.05$, ××× $p<0.001$, ×××× $p<0.0001$ compared to the CC-4533 strain. µE stands for µmole photons m^{-2} s^{-1}.

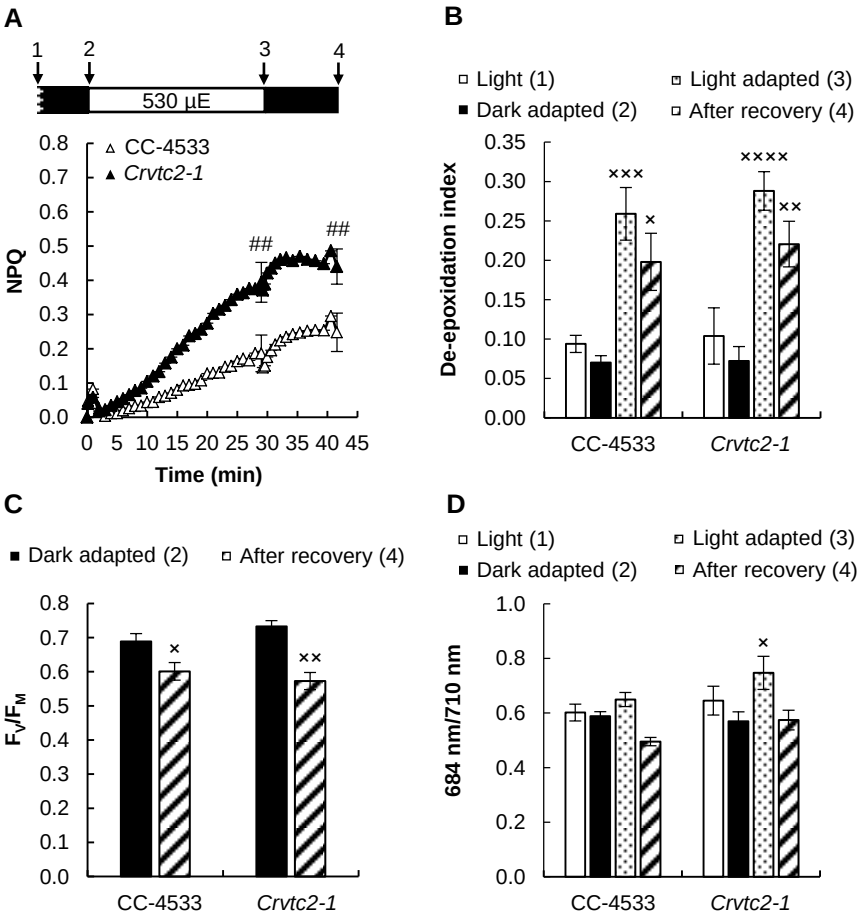

Figure 3 – Acclimation to 530 µmole photons m^{-2} s^{-1} of red light followed by recovery in CC-4533 (wild type) and *Crvtc2-1* cultures, grown photomixotrophically in TAP medium at 100 µmole photons m^{-2} s^{-1}. A, NPQ kinetics; B, De-epoxidation index; C, F_V/F_M parameter measured after dark adaptation and after recovery from the 530 µmole photons m^{-2} s^{-1} red light; D, 684 nm/ 710 nm ratio of the 77K fluorescence spectra. Samples were collected at the growth light of 100 µmole photons m^{-2} s^{-1}, after 30 min of dark-adaptation, at the end of the 30 min light period to 530 µmole photons m^{-2} s^{-1} and 15 min after the cessation of actinic illumination, as indicated by arrows in the scheme in panel A. Data was analyzed by one-way ANOVA followed by Dunnett post-test: ## $p<0.01$ compared to the CC-4533 strain at the respective time-point; × $p<0.05$, ×× $p<0.01$, ××× $p<0.001$ compared to the dark-adapted CC-4533 strain. µE stands for µmole photons m^{-2} s^{-1}.

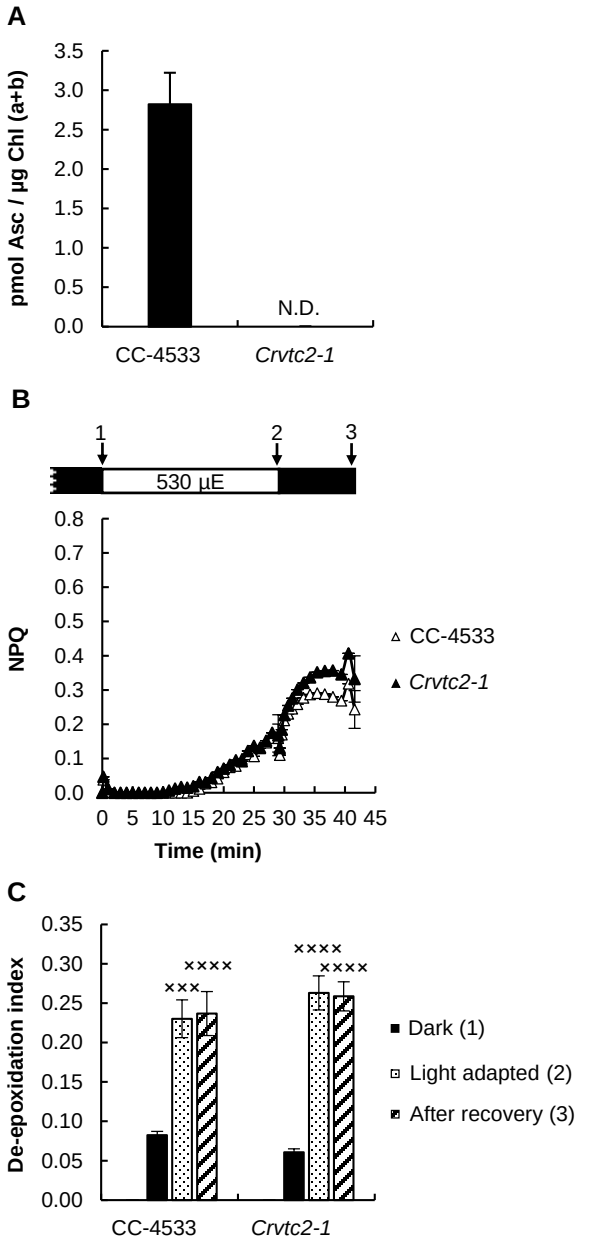

Figure 4 – Effects of overnight (16 h) dark acclimation on the CC-4533 and the *Crvtc2-1* (grown in TAP medium at 100 µmole photons m^{-2} s^{-1}). A, Ascorbate content after 16 h of dark acclimation; B, NPQ, induced by 530 µmole photons m^{-2} s^{-1} of red light after overnight dark acclimation; C, de-epoxidation index, determined in the overnight dark-acclimated cultures, after strong red-light illumination and following recovery. Data was analyzed by one-way ANOVA followed by Dunnett post-test: ××× $p<0.001$, ×××× $p<0.0001$ compared to the dark-acclimated CC-4533 strain. µE stands for µmole photons m^{-2} s^{-1}.

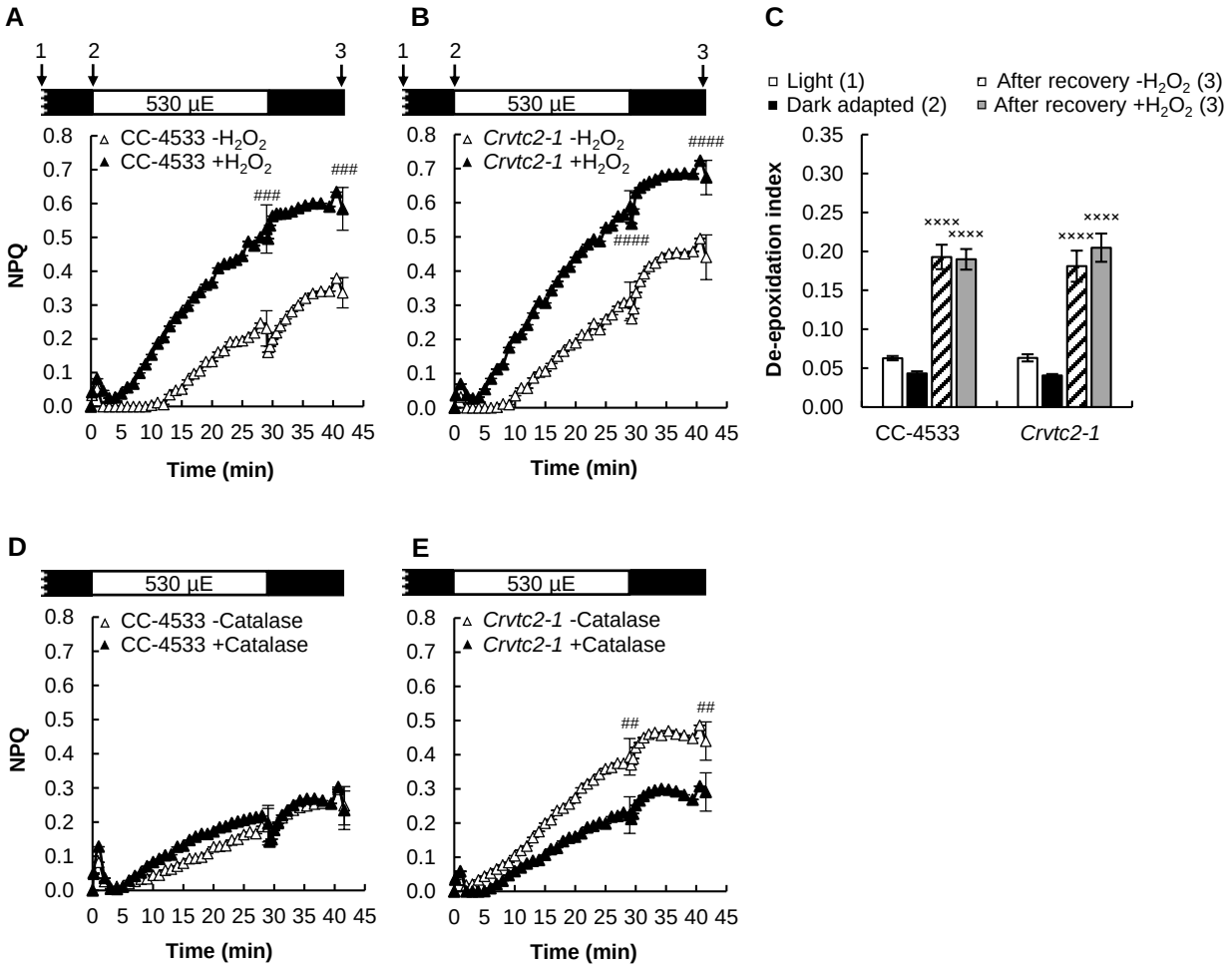

Figure 5 – The effects of H_2O_2 and catalase on NPQ, induced by strong red light (530 µmole photons m^{-2} s^{-1}) in the wild type (CC-4533) and the *Crvtc2-1* mutant grown in photomixotrophic conditions in TAP medium at 100 µmole photons m^{-2} s^{-1}. A, The effect of 1.5 mM H_2O_2 on NPQ induction in the CC-4533 strain; B, the effect of 1.5 mM H_2O_2 on NPQ induction in the *Crvtc2-1* mutant; C, the effect of H_2O_2 addition on de-epoxidation; D, the effect of catalase on NPQ induction in the CC-4533 strain; E, the effect of catalase on NPQ induction in the *Crvtc2-1* mutant. Samples were collected at the time points indicated by arrows in the schemes in panels A and B. Data was analyzed by one-way ANOVA followed by Dunnett post-test: ## p<0.01, ### p<0.001, #### p<0.0001 compared to the untreated CC-4533 culture at the respective time-point; × p<0.05, ×× p<0.01, ××× p<0.001 compared to the dark-adapted CC-4533 strain. µE stands for µmole photons m^{-2} s^{-1}.

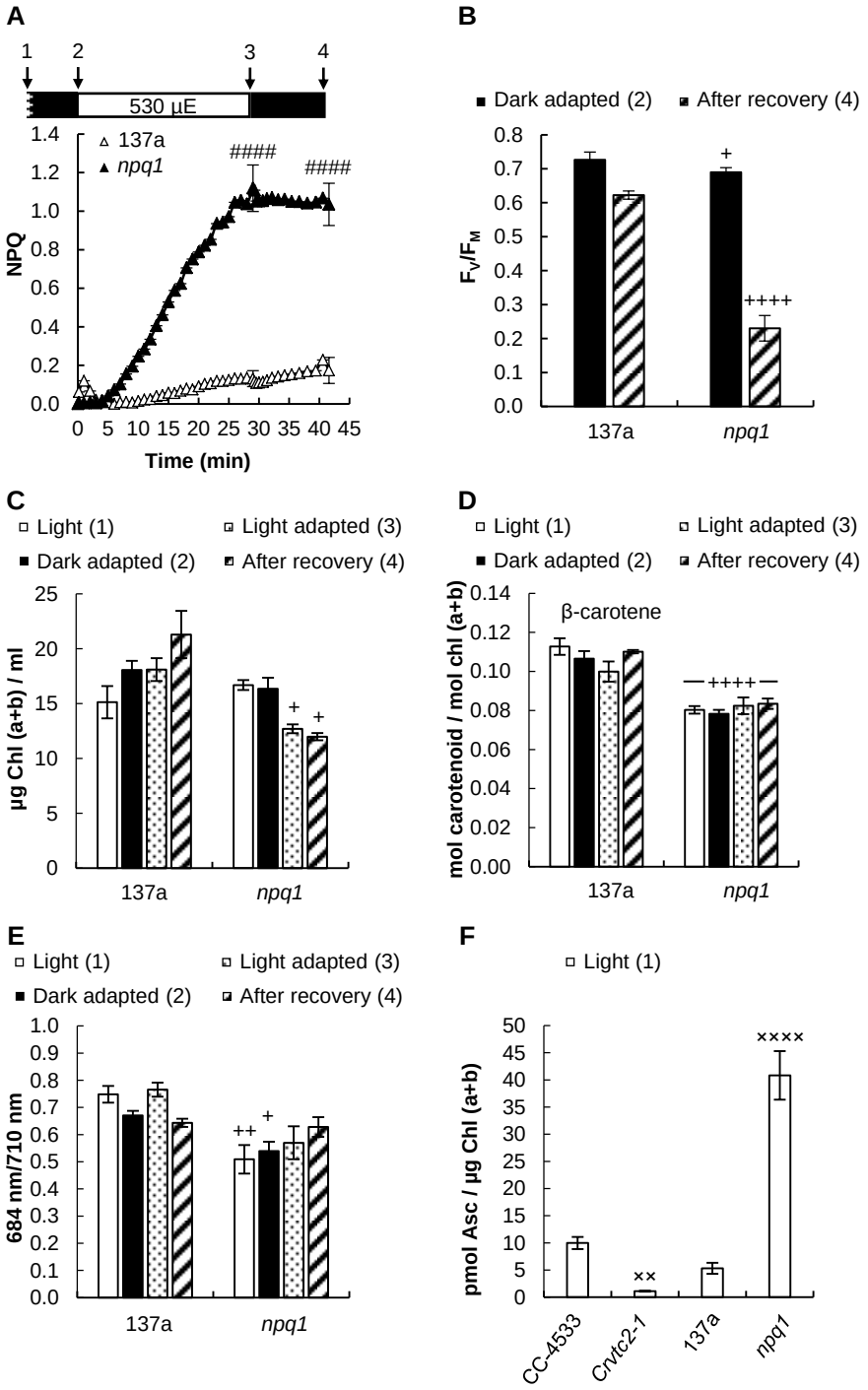

Figure 6 – Effects of strong red light (530 µmole photons m^{-2} s^{-1}) on the 137a (wild type) and the *npq1* mutant of *C. reinhardtii* grown in TAP medium at 100 µmole photons m^{-2} s^{-1}. A, NPQ induced by 530 µmole photons m^{-2} s^{-1} of red light followed by a recovery phase; B, F_V/F_M value, determined before the strong red light illumination and after the recovery phase; C, Chl(a+b) content of the cultures determined before, during and after the strong red light illumination; D, β-carotene content measured before, during and after the strong red light illumination; E, 684 nm/ 710 nm ratio of the 77K fluorescence spectra determined before, during and after the strong red light illumination; F, Ascorbate contents of the *npq1* and *Crvtc2-1* mutants and the CC-4533 and 137a wild type strains. Samples were collected at the time points indicated by arrows in the scheme in panel A. Data was analyzed by one-way ANOVA followed by Dunnett post-test: #### p<0.0001 compared to the 137a strain at the respective time-point; + p<0.05, ++ p<0.01, ++++ p<0.0001 compared to the dark-adapted 137a strain; ×× p<0.01, ×××× p<0.0001 compared to the CC-4533 strain. µE stands for µmole photons m^{-2} s^{-1}.

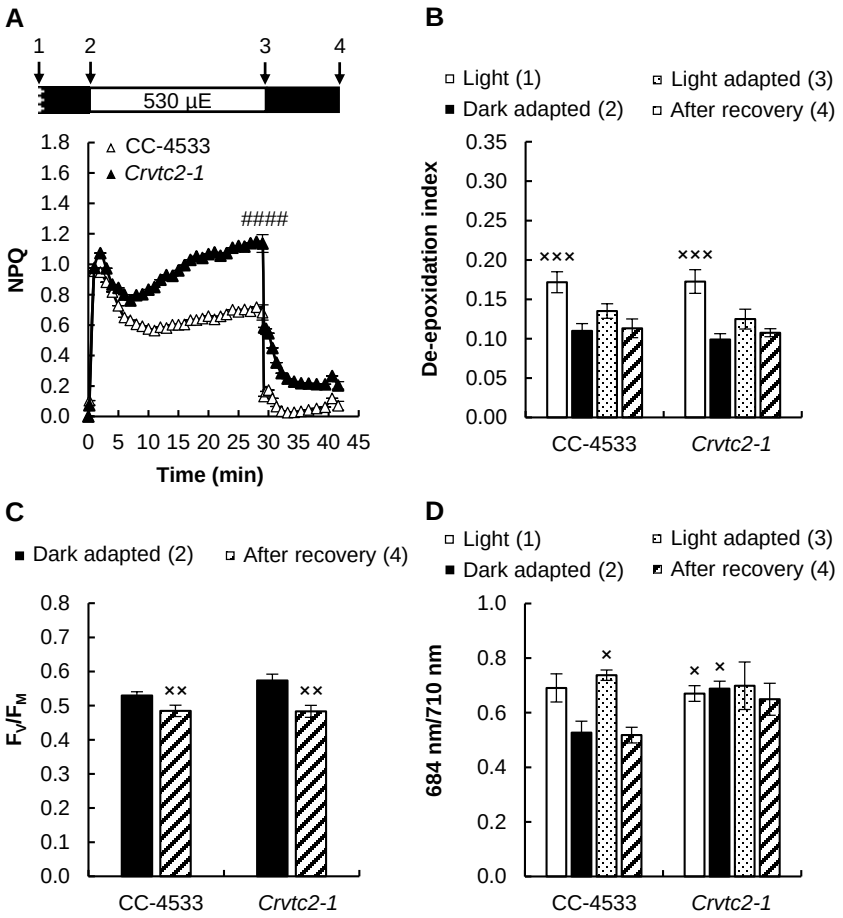

Figure 7 – Acclimation to 530 µmole photons m^{-2} s^{-1} of red light followed by recovery in CC-4533 and *Crvtc2-1* cultures, grown photoautotrophically in HSM medium at 530 µmole photons m^{-2} s^{-1}. A, NPQ kinetics; B, De-epoxidation index; C, F_V/F_M parameter measured after dark adaptation and after recovery from the 530 µmole photons m^{-2} s^{-1} red light illumination; D, 684 nm/ 710 nm ratio of the 77K fluorescence spectra. The samples were collected at the growth light of 530 µmole photons m^{-2} s^{-1}, after 30 min of dark adaptation, at the end of the 30 min red light illumination, and 12 min after the cessation of actinic illumination, as indicated in the scheme in panel A. Data was analyzed by one-way ANOVA followed by Dunnett post-test: #### $p<0.0001$ compared to the CC-4533 strain at the respective time-point; × $p<0.05$, ×× $p<0.01$, ××× $p<0.001$ compared to the dark-adapted CC-4533 strain. µE stands for µmole photons m^{-2} s^{-1}.

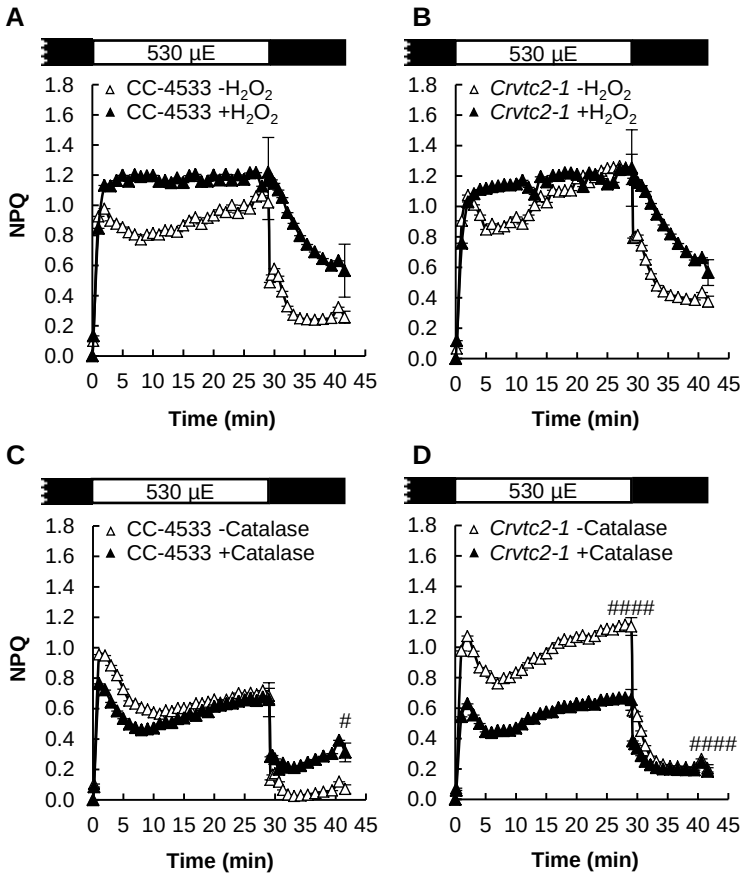

Figure 8 – The effects of H_2O_2 and catalase on NPQ induced by strong red light (530 µmole photons m^{-2} s^{-1}) in the wild type (CC-4533) and *Crvtc2-1* mutant strains grown photoautotrophically in HSM medium at 530 µmole photons m^{-2} s^{-1}. A, The effect of 1.5 mM H_2O_2 on NPQ induction in the CC-4533 strain; B, the effect of 1.5 mM H_2O_2 on NPQ induction in the *Crvtc2-1* mutant; C, the effect of catalase on NPQ induction in the CC-4533 strain; D, the effect of catalase on NPQ induction in the *Crvtc2-1* mutant. Data was analyzed by one-way ANOVA followed by Dunnett post-test: # $p<0.05$, #### $p<0.0001$ compared to the untreated CC-4533 culture at the respective time-point. µE stands for µmole photons m^{-2} s^{-1}.

Parsed Citations

Adams WW III, Muller O, Cohu CM, Demmig-Adams B (2013) May photoinhibition be a consequence, rather than a cause, of limited plant productivity? Photosynth Res 117:31-44
Pubmed: Author and Title
Google Scholar: Author Only Title Only Author and Title

Allorent G, Tokutsu R, Roach T, Peers G, Cardol P, Girard-Bascou J, Seigneurin-Berny D, Petroutsos D, Kuntz M, Breyton C, Franck F, Wollman FA, Niyogi KK, Krieger-Liszkay A, Minagawa J, Finazzi G (2013) A dual strategy to cope with high light in Chlamydomonas reinhardtii. Plant Cell 25:545-557
Pubmed: Author and Title
Google Scholar: Author Only Title Only Author and Title

Anwaruzzaman M, Chin BL, Li X-P, Lohr M, Martinez DA, Niyogi KK (2004) Genomic analysis of mutants affecting xanthophyll biosynthesis and regulation of photosynthetic light harvesting in Chlamydomonas reinhardtii. Photosynth Res 82:265-276
Pubmed: Author and Title
Google Scholar: Author Only Title Only Author and Title

Arnoux P, Morosinotto T, Saga G, Bassi R, Pignol D (2009) A structural basis for the pH-dependent xanthophyll cycle in Arabidopsis thaliana. Plant Cell 21: 2036-2044
Pubmed: Author and Title
Google Scholar: Author Only Title Only Author and Title

Asada K (2006) Production and scavenging of reactive oxygen species in chloroplasts and their functions. Plant Physiol 141: 391-396
Pubmed: Author and Title
Google Scholar: Author Only Title Only Author and Title

Avenson TJ, Ahn TK, Zigmantas D, Niyogi KK, Li Z, Ballottari M, Bassi R, Fleming GR (2008) Zeaxanthin radical cation formation in minor light-harvesting complexes of higher plant antenna. J Biol Chem 283:3550-3558
Pubmed: Author and Title
Google Scholar: Author Only Title Only Author and Title

Azzabi G, Pinnola A, Betterle N, Bassi R, Alboresi A (2012) Enhancement of non-photo de-epoxidation index chemical quenching in the bryophyte Physcomitrella patens during acclimation to salt and osmotic stress. Plant Cell Physiol 53: 1815-1825
Pubmed: Author and Title
Google Scholar: Author Only Title Only Author and Title

Barahimipour R, Strenkert D, Neupert J, Schroda M, Merchant SS, Bock R (2015) Dissecting the contributions of GC content and codon usage to gene expression in the model alga Chlamydomonas reinhardtii. Plant J 84: 704-717
Pubmed: Author and Title
Google Scholar: Author Only Title Only Author and Title

Baroli I, Do AD, Yamane T, Niyogi KK (2003) Zeaxanthin accumulation in the absence of a functional xanthophyll cycle protects Chlamydomonas reinhardtii from photooxidative stress. Plant Cell 15: 992-1008
Pubmed: Author and Title
Google Scholar: Author Only Title Only Author and Title

Bratt C, Arvidsson P, Carlsson M, Akerlund H (1995) Regulation of violaxanthin de-epoxidase activity by pH and ascorbate. Photosynth Res 45: 169-175
Pubmed: Author and Title
Google Scholar: Author Only Title Only Author and Title

Bonente G, Ballottari M, Truong T, Morosinotto T, Ahn T, Fleming G, Niyogi K, Bassi R (2011) Analysis of LhcSR3, a protein essential for feedback de- excitation in the green alga Chlamydomonas reinhardtii. PLoS Biol 9:e1000577
Pubmed: Author and Title
Google Scholar: Author Only Title Only Author and Title

Bradbury LMT, Shumskaya M, Tzfadia O, Wu S-B, Kennelly EK, Wurtzelt ET (2012) Lycopene cyclase paralog CruP protects against reactive oxygen species in oxygenic photosynthetic organisms. Proc Natl Acad Sci USA 109:E1888-E1897
Pubmed: Author and Title
Google Scholar: Author Only Title Only Author and Title

Chaux F, Johnson X, Auroy P, Beyly-Adriano A, Te I, Cuiné S, Peltier G (2017) PGRL1 and LHCSR3 compensate for each other in controlling photosynthesis and avoiding photosystem I photoinhibition during high light acclimation of Chlamydomonas cells. Mol Plant 10:216-218
Pubmed: Author and Title
Google Scholar: Author Only Title Only Author and Title

Christa G, Cruz S, Jahns P, de Vries J, Cartaxana P, Esteves AC, Serôdio J, Gould SB (2017) Photoprotection in a monophyletic branch of chlorophyte algae is independent of energy-dependent quenching (qE). New Phytol 214: 1132-1144
Pubmed: Author and Title
Google Scholar: Author Only Title Only Author and Title

Depège N, Bellafiore S, Rochaix JD (2003) Role of chloroplast protein kinase Stt7 in LHCII phosphorylation and state transition in

Chlamydomonas. Science 299: 1572-1575
Pubmed: Author and Title
Google Scholar: Author Only Title Only Author and Title

Dowdle J, Ishikawa T, Gatzek S, Rolinski S, Smirnoff N (2007) Two genes in Arabidopsis thaliana encoding GDP-L-galactose phosphorylase are required for ascorbate biosynthesis and seedling viability. Plant J 52: 673-689
Pubmed: Author and Title
Google Scholar: Author Only Title Only Author and Title

Erickson E, Wakao S, Niyogi KK (2015) Light stress and photoprotection in Chlamydomonas reinhardtii. Plant J 82:449-465
Pubmed: Author and Title
Google Scholar: Author Only Title Only Author and Title

Fernie AR, Tóth SZ (2015) Identification of the elusive chloroplast ascorbate transporter extends the substrate specificity of the PHT family. Mol Plant 8:674-676
Pubmed: Author and Title
Google Scholar: Author Only Title Only Author and Title

Finazzi G, Johnson GN, Dall'Osto L, Zito F, Bonente G, Bassi R, Wollman F-A (2006) Nonphotochemical quenching of chlorophyll fluorescence in Chlamydomonas reinhardtii. Biochemistry 45:1490-1498
Pubmed: Author and Title
Google Scholar: Author Only Title Only Author and Title

Foyer CH, Shigeoka S (2011) Understanding oxidative stress and antioxidant functions to enhance photosynthesis. Plant Physiol 155: 93-100
Pubmed: Author and Title
Google Scholar: Author Only Title Only Author and Title

Gest N, Gautier H, Stevens R (2013) Ascorbate as seen through plant evolution: the rise of a successful molecule? J Exp Bot 64:33-53
Pubmed: Author and Title
Google Scholar: Author Only Title Only Author and Title

Grouneva I, Jakob T, Wilhelm C, Goss R (2006) Influence of ascorbate and pH on the activity of the diatom xanthophyll cycle-enzyme diadinoxanthin de-epoxidase. Physiol Plant 126:205-211
Pubmed: Author and Title
Google Scholar: Author Only Title Only Author and Title

Hager A, Holocher K (1994) Localization of the xanthophyll-cycle enzyme violaxanthin de-epoxidase within the thylakoid lumen and abolition of its mobility by a (light-dependent) pH decrease. Planta 192: 581-589
Pubmed: Author and Title
Google Scholar: Author Only Title Only Author and Title

Hallin EI, Hasan M, Guo K, Åkerlund H-E (2016) Molecular studies on structural changes and oligomerisation of violaxanthin de-epoxidase associated with the pH-dependent activation. Photosynth Res 129: 29-41
Pubmed: Author and Title
Google Scholar: Author Only Title Only Author and Title

Hieber AD, Bugos RC, Yamamoto HY (2000) Plant lipocalins: violaxanthin de-epoxidase and zeaxanthin epoxidase. Biochim Biophys Acta BBA - Protein Struct Mol Enzymol 1482: 84-91
Pubmed: Author and Title
Google Scholar: Author Only Title Only Author and Title

Holt NE, Zigmantas D, Valkunas L, Li X-P, Niyogi KK, Fleming GR (2005) Carotenoid cation formation and the regulation of photosynthetic light harvesting. Science 307:433-436
Pubmed: Author and Title
Google Scholar: Author Only Title Only Author and Title

Holub O, Seufferheld MJ, Gohlke C, Heiss GJ, Clegg RM (2007) Fluorescence lifetime imaging microscopy of Chlamydomonas reinhardtii: non-photochemical quenching mutants and the effect of photosynthetic inhibitors on the slow chlorophyll fluorescence transient. J Microsc 226: 90-120
Pubmed: Author and Title
Google Scholar: Author Only Title Only Author and Title

Ivanov B, Asada K, Edwards GE (2007) Analysis of donors of electrons to photosystem I and cyclic electron flow by redox kinetics of P700 in chloroplasts of isolated bundle sheath strands of maize. Photosynth Res 92:65-74
Pubmed: Author and Title
Google Scholar: Author Only Title Only Author and Title

Iwai M, Kato N, Minagawa J (2007) Distinct physiological responses to a high light and low CO2 environment revealed by fluorescence quenching in photoautotrophically grown Chlamydomonas reinhardtii. Photosynth Res 94:307-314
Pubmed: Author and Title
Google Scholar: Author Only Title Only Author and Title

Jeffrey SW, Mantoura RFC, Wright SW (1997) Phytoplankton pigments in oceanography: guidelines to modern methods. (Paris: UNESCO Publishing)

Pubmed: Author and Title
Google Scholar: Author Only Title Only Author and Title

Johnson X, Alric J (2012) Interaction between starch breakdown, acetate assimilation, and photosynthetic cyclic electron flow in Chlamydomonas reinhardtii. J Biol Chem 287:26445-26452
Pubmed: Author and Title
Google Scholar: Author Only Title Only Author and Title

Johnson MP, Davison PA, Ruban AV, Horton P (2008) The xanthophyll cycle pool size controls the kinetics of non-photochemical quenching in Arabidopsis thaliana. FEBS Lett 582:259-263
Pubmed: Author and Title
Google Scholar: Author Only Title Only Author and Title

Kanazawa A, Kramer DM (2002). In vivo modulation of nonphotochemical exciton quenching (NPQ) by regulation of the chloroplast ATP synthase. Proc Natl Acad Sci USA 99:12789-12794
Pubmed: Author and Title
Google Scholar: Author Only Title Only Author and Title

Kovács L, Vidal-Meireles A, Nagy V, Tóth SZ (2016) Quantitative determination of ascorbate from the green alga Chlamydomonas reinhardtii by HPLC. Bio-Protoc 6:e2067
Pubmed: Author and Title
Google Scholar: Author Only Title Only Author and Title

Lemeille S, Willig A, Depège-Fargeix N, Delessert C, Bassi R, Rochaix J-D (2009) Analysis of the chloroplast protein kinase Stt7 during state transitions. PLoS Biol 7: e1000045
Pubmed: Author and Title
Google Scholar: Author Only Title Only Author and Title

Li S, Liu L, Zhuang X, Yu Y, Liu X, Cui X, Ji L, Pan Z, Cao X, Mo B, Zhang F, Raikhel N, Jiang L, and Chen X (2013) MicroRNAs inhibit the Ttranslation of target mRNAs on the endoplasmic reticulum in Arabidopsis. Cell 153: 562-574
Pubmed: Author and Title
Google Scholar: Author Only Title Only Author and Title

Li Z, Peers G, Dent RM, Bai Y, Yang SY, Apel W, Leonelli L, Niyogi KK (2016a) Evolution of an atypical de-epoxidase for photoprotection in the green lineage. Nat Plants 2: 16140
Pubmed: Author and Title
Google Scholar: Author Only Title Only Author and Title

Li X, Zhang R, Patena W, Gang SS, Blum SR, Ivanova N, Yue R, Robertson JM, Lefebvre PA, Fitz-Gibbon ST, Grossman AR, Jonikas MC (2016b) An indexed, mapped mutant library enables reverse genetics studies of biological processes in Chlamydomonas reinhardtii. Plant Cell 28: 367-387
Pubmed: Author and Title
Google Scholar: Author Only Title Only Author and Title

Marschall M, Proctor MCF (2004) Are bryophytes shade plants? Photosynthetic light responses and proportions of chlorophyll a, chlorophyll b and total carotenoids. Ann Bot 94: 593-603
Pubmed: Author and Title
Google Scholar: Author Only Title Only Author and Title

Müller-Moulé P, Conklin PL, Niyogi KK (2002) Ascorbate deficiency can limit violaxanthin de-epoxidase activity in vivo. Plant Physiol 128: 970-977
Pubmed: Author and Title
Google Scholar: Author Only Title Only Author and Title

Müller-Moulé P, Havaux M, Niyogi KK (2003) Zeaxanthin deficiency enhances the high light sensitivity of an ascorbate-deficient mutant of Arabidopsis. Plant Physiol 133: 748-760.
Pubmed: Author and Title
Google Scholar: Author Only Title Only Author and Title

Nagy V, Vidal-Meireles A, Podmaniczki A, Szentmihályi K, Rákhely G, Zsigmond L, Kovács L, Tóth SZ (2018) The mechanism of photosystem II inactivation during sulphur deprivation-induced H2 production in Chlamydomonas reinhardtii. Plant J 94:548-561
Pubmed: Author and Title
Google Scholar: Author Only Title Only Author and Title

Neupert J, Karcher D, Bock R (2009) Generation of Chlamydomonas strains that efficiently express nuclear transgenes. Plant J 57:1140-1150
Pubmed: Author and Title
Google Scholar: Author Only Title Only Author and Title

Niyogi KK, Bjorkman O, Grossmann AR (1997) Chlamydomonas xanthophyll cycle mutants identified by video imaging of chlorophyll fluorescence quenching. Plant Cell 9:1369-1380
Pubmed: Author and Title
Google Scholar: Author Only Title Only Author and Title

Peers G, Truong TB, Ostendorf E, Busch A, Elrad D, Grossman AR, Hippler M, Niyogi KK (2009) An ancient light-harvesting protein is

critical for the regulation of algal photosynthesis. Nature 462:518-521
Pubmed: Author and Title
Google Scholar: Author Only Title Only Author and Title

Pinnola A, Dall'Osto L, Gerotto C, Morosinotto T, Bassi R, Alboresi A (2013) Zeaxanthin binds to Light-Harvesting Complex Stress-Related Protein to enhance nonphotochemical quenching in Physcomitrella patens. Plant Cell 25:3519-3534
Pubmed: Author and Title
Google Scholar: Author Only Title Only Author and Title

Polukhina I, Fristedt R, Dinc E, Cardol P, Croce R (2016) Carbon supply and photoacclimation cross talk in the green alga Chlamydomonas reinhardtii. Plant Physiol 172: 1494-1505
Pubmed: Author and Title
Google Scholar: Author Only Title Only Author and Title

Porra RJ, Thompson WA, Kriedeman PE (1989) Determination of accurate extinction coefficients and simultaneous equations for essaying chlorophylls-a and -b with four different solvents: verification of the concentration of chlorophyll standards by atomic absorption spectroscopy. Biochim Biophys Acta 975: 384-394
Pubmed: Author and Title
Google Scholar: Author Only Title Only Author and Title

Quaas T, Berteotti S, Ballottari M, Flieger K, Bassi R, Wilhelm C, Goss R (2015) Non-photochemical quenching and xanthophyll cycle activities in six green algal species suggest mechanistic differences in the process of excess energy dissipation. J. Plant Physiol 172: 92-103
Pubmed: Author and Title
Google Scholar: Author Only Title Only Author and Title

Roach T, Na CS (2017) LHCSR3 affects de-coupling and re-coupling of LHCII to PSII during state transitions in Chlamydomonas reinhardtii. Sci Rep 7: 43145
Pubmed: Author and Title
Google Scholar: Author Only Title Only Author and Title

Ruban AV, Johnson MP, Duffy CD (2012) The photoprotective molecular switch in the photosystem II antenna. Biochim Biophys Acta 1817:167-181
Pubmed: Author and Title
Google Scholar: Author Only Title Only Author and Title

Saga G, Giorgetti A, Fufezan C, Giacometti GM, Bassi R, Morosinotto T (2010) Mutation analysis of violaxanthin de-epoxidase identifies substrate-binding sites and residues involved in catalysis. J Biol Chem 285:23763-23770
Pubmed: Author and Title
Google Scholar: Author Only Title Only Author and Title

Schroda M, Vallon O, Whitelegge JP, Beck CF, Wollman FA (2001) The chloroplastic GrpE homolog of Chlamydomonas: two isoforms generated by differential splicing. Plant Cell 13:2823-2839
Pubmed: Author and Title
Google Scholar: Author Only Title Only Author and Title

Smirnoff N (2018) Ascorbic acid metabolism and functions: A comparison of plants and mammals. Free Radic Biol Med. 122:116-129
Pubmed: Author and Title
Google Scholar: Author Only Title Only Author and Title

Takizawa K, Kanazawa A, Kramer DM (2008) Depletion of stromal Pi induces high 'energy dependent' antenna exciton quenching (qE) by decreasing proton conductivity at CFO-CF1 ATP synthase. Plant Cell Environ 31:235-243
Pubmed: Author and Title
Google Scholar: Author Only Title Only Author and Title

Tibiletti T, Auroy P, Peltier G, Caffarri S (2016) Chlamydomonas reinhardtii PsbS protein is functional and accumulates rapidly and transiently under high light. Plant Physiol 171:2717-2730
Pubmed: Author and Title
Google Scholar: Author Only Title Only Author and Title

Tikkanen M, Mekala NR, Aro E-M (2014) Photosystem II photoinhibition-repair cycle protects photosystem I from irreversible damage. Biochim Biophys Acta - Bioenerg 1837: 210-215
Pubmed: Author and Title
Google Scholar: Author Only Title Only Author and Title

Tóth SZ, Puthur JT, Nagy V, Garab G (2009) Experimental evidence for ascorbate-dependent electron transport in leaves with inactive oxygen-evolving complexes. Plant Physiol 149: 1568-1578
Pubmed: Author and Title
Google Scholar: Author Only Title Only Author and Title

Tóth SZ, Nagy V, Puthur JT, Kovács L, Garab G (2011) The physiological role of ascorbate as photosystem II electron donor: Protection against photoinactivation in heat-stressed leaves. Plant Physiol 156: 382-392
Pubmed: Author and Title
Google Scholar: Author Only Title Only Author and Title

Tóth SZ, Lőrincz T, Szarka A (2018) Concentration does matter: The beneficial and potentially harmful effects of ascorbate in humans and plants. Antioxid Redox Signal 29:1516-1533
Pubmed: Author and Title
Google Scholar: Author Only Title Only Author and Title

Ünlü C, Drop B, Croce R, van Amerongen H (2014) State transitions in Chlamydomonas reinhardtii strongly modulate the functional size of photosystem II but not of photosystem I. Proc Natl Acad Sci USA 111:3460-3465
Pubmed: Author and Title
Google Scholar: Author Only Title Only Author and Title

Urzica EI, Adler LN, Page MD, Linster CL, Arbing MA, Casero D, Pellegrini M, Merchant SS, Clarke SG (2012) Impact of oxidative stress on ascorbate biosynthesis in Chlamydomonas via regulation of the VTC2 gene encoding a GDP-L-galactose phosphorylase. J Biol Chem 287: 14234-14245
Pubmed: Author and Title
Google Scholar: Author Only Title Only Author and Title

Vidal-Meireles A, Neupert J, Zsigmond L, Rosado-Souza L, Kovács L, Nagy V, Galambos A, Fernie AR, Bock R, Tóth SZ (2017) Regulation of ascorbate biosynthesis in green algae has evolved to enable rapid stress-induced response via the VTC2 gene encoding GDP- L -galactose phosphorylase. New Phytol 214: 668-681
Pubmed: Author and Title
Google Scholar: Author Only Title Only Author and Title

Voigt J, Münzner P (1994) Blue light-induced lethality of a cell wall-deficient mutant of the unicellular green alga Chlamydomonas reinhardtii. Plant Cell Physiol 35: 99-106
Pubmed: Author and Title
Google Scholar: Author Only Title Only Author and Title

Wang Z, Xiao Y, Chen W, Tang K, Zhang L (2010) Increased vitamin C content accompanied by an enhanced recycling pathway confers oxidative stress tolerance in Arabidopsis. J. Integr. Plant Biol 52: 400-409
Pubmed: Author and Title
Google Scholar: Author Only Title Only Author and Title

Wheeler G, Ishikawa T, Pornsaksit V, Smirnoff N (2015) Evolution of alternative biosynthetic pathways for vitamin C following plastid acquisition in photosynthetic eukaryotes. eLife 4:e06369
Pubmed: Author and Title
Google Scholar: Author Only Title Only Author and Title

Xue H, Tokutsu R, Bergner SV, Scholz M, Minagawa J, Hippler M (2015) Photosystem II subunit R is required for efficient binding of Light-Harvesting Complex Stress-Related Protein 3 to photosystem II-light-harvesting supercomplexes in Chlamydomonas reinhardtii. Plant Physiol 167: 1566-1578
Pubmed: Author and Title
Google Scholar: Author Only Title Only Author and Title

Zechmann B, Stumpe M, Mauch F (2011) Immunocytochemical determination of the subcellular distribution of ascorbate in plants. Planta 233: 1-12
Pubmed: Author and Title
Google Scholar: Author Only Title Only Author and Title